





Review

The “Forgotten” Hydroxyapatite Crystals in Regenerative Bone Tissue Engineering: A Critical Review

Anastasios-Nektarios Tzavellas ^{1,2}, Chrysoula Katrilaka ³, Niki Karipidou ³, Magdalini Kanari ³, Maria Pitou ⁴, Georgios Koliakos ⁵, Angeliki Cheva ⁶, Theodora Choli-Papadopoulou ⁴, Amalia Aggeli ^{3,*} and Eleftherios Tsiridis ^{2,7}

- ¹ 1st Orthopaedic and Trauma Department, 424 Military General Hospital of Thessaloniki, 56429 Thessaloniki, PC, Greece; tzavellas.ortho@gmail.com
 - ² Center of Orthopaedics and Regenerative Medicine (C.O.RE.), Center of Interdisciplinary Research and Innovation (C.I.R.I.), Aristotle University of Thessaloniki, Balkan Center, 57001 Thessaloniki, PC, Greece; tsiridis@sehs@gmail.com
 - ³ Department of Chemical Engineering, School of Engineering, Aristotle University of Thessaloniki, University Campus, 54124 Thessaloniki, PC, Greece; chrysoulakatrilaka@gmail.com (C.K.); nickykar7@gmail.com (N.K.); magdalini.kanari@gmail.com (M.K.)
 - ⁴ School of Chemistry, Aristotle University of Thessaloniki, University Campus, 54124 Thessaloniki, PC, Greece; pitoumaria91@gmail.com (M.P.); tcholi@chem.auth.gr (T.C.-P.)
 - ⁵ Laboratory of Biochemistry, School of Medicine, Aristotle University of Thessaloniki, University Campus, 54124 Thessaloniki, PC, Greece; koliakos@yahoo.gr
 - ⁶ Laboratory of Pathology, School of Medicine, Aristotle University of Thessaloniki, University Campus, 54124 Thessaloniki, PC, Greece; antacheva@yahoo.gr
 - ⁷ 3rd Academic Orthopaedic Department, Papageorgiou General Hospital, School of Medicine, Aristotle University of Thessaloniki, 56429 Thessaloniki, PC, Greece
- * Correspondence: aggeli@cheng.auth.gr; Tel.: +30-697-742-6376



Citation: Tzavellas, A.-N.; Katrilaka, C.; Karipidou, N.; Kanari, M.; Pitou, M.; Koliakos, G.; Cheva, A.; Choli-Papadopoulou, T.; Aggeli, A.; Tsiridis, E. The “Forgotten” Hydroxyapatite Crystals in Regenerative Bone Tissue Engineering: A Critical Review. *Crystals* **2024**, *14*, 448. <https://doi.org/10.3390/cryst14050448>

Academic Editor: José L. Arias

Received: 6 April 2024

Revised: 24 April 2024

Accepted: 4 May 2024

Published: 8 May 2024



Copyright: © 2024 by the authors. Licensee MDPI, Basel, Switzerland. This article is an open access article distributed under the terms and conditions of the Creative Commons Attribution (CC BY) license (<https://creativecommons.org/licenses/by/4.0/>).

Abstract: Bone regeneration using Bone Morphogenetic Proteins (BMPs) alongside various engineered scaffolds has attracted considerable attention over the years. The field has seen extensive research in preclinical animal models, leading to the approval of two products and guiding the quest for new materials. Natural and synthetic polymers, ceramics, and composites have been used to fabricate the necessary porous 3D scaffolds and delivery systems for BMPs. Interestingly, all reported applications in the literature are triumphant. Evaluation of the results is typically based on histologic assessment after appropriate staining and radiological modalities, providing morphological identification of the newly formed bone and describing cells and the organic compound. Remarkably, while these evaluation methods illustrate mineralization, they are not capable of identifying hydroxyapatite crystals, the mineral component of the bone, which are crucial for its mechanical properties, structure, integrity, and long-term stability of regenerated bone tissue. This review aims to focus on the different scaffolds used in bone tissue engineering applications and underline the pressing need for techniques that could recognize the presence of hydroxyapatite crystals as well as their characteristics in bone tissue engineering, which will provide a more complete and comprehensive assessment of the successful results.

Keywords: bone tissue engineering; scaffold; bone morphogenetic protein; calcium phosphate; hydroxyapatite crystals; characterization techniques

1. Introduction

Bone is a unique tissue, consisting of cells, alongside the organic and inorganic parts of its matrix (Figure 1). Type I collagen is the main organic component, providing structural support and flexibility, whereas hydroxyapatite crystals (HA) primarily form the inorganic phase, imparting strength and rigidity to bone tissue. Hydroxyapatite is a member of the

Calcium Phosphates (CaP) family, a group of minerals found in many living organisms, further highlighting its fundamental role in biological systems.

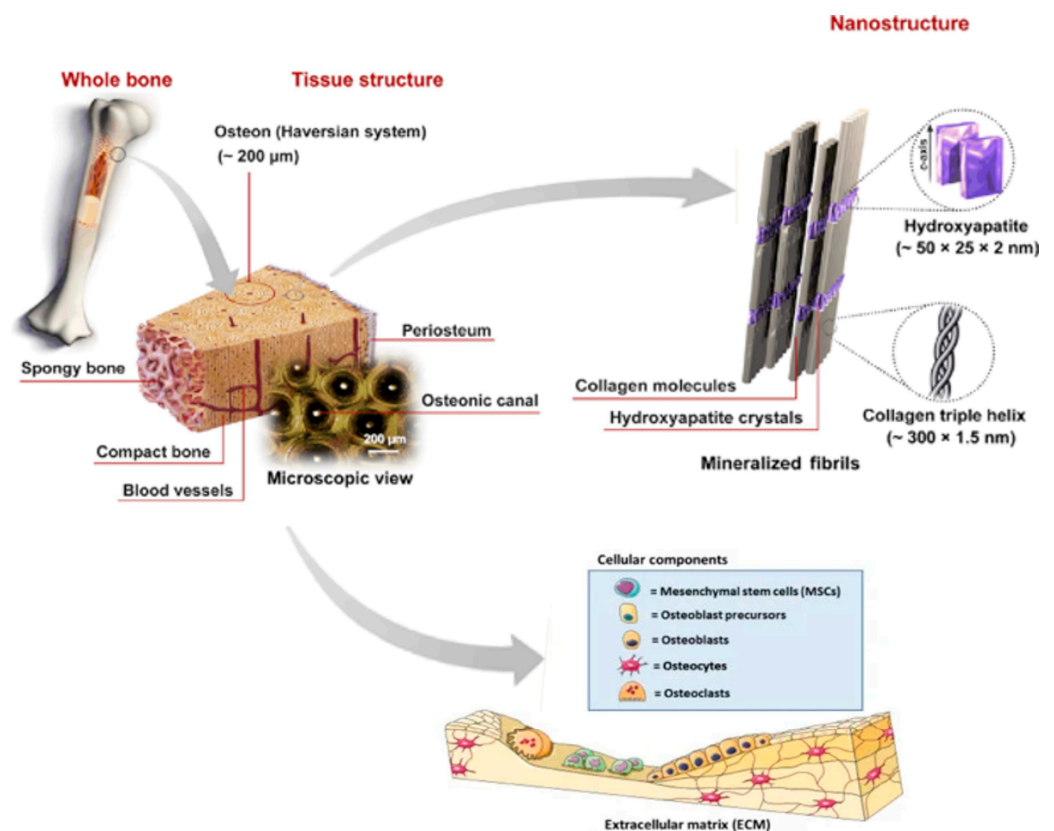


Figure 1. Typical structure of bone, showing cellular components and extracellular matrix with its organic and inorganic compounds, modified from [1,2]. Adapted with permission from Ref. [1]. 2013, Elsevier Ltd., Amsterdam, The Netherlands.

Bone tissue exists in an impressive dynamic equilibrium with exceptional capability for regeneration and remodeling. It is able to fully restore its functional and structural characteristics following an injury. Despite that, delayed union and pseudarthrosis can happen as often as up to 10% [3–5]. Additionally, the surgical treatment of open fractures, infection and osteomyelitis, and cancer can create the challenge of coverage of large bone defects. Traditionally, a bone graft is the main option with autologous grafting being the “gold standard”. An alternative approach includes the use of materials, cells and growth factors in an attempt to produce bone either ectopically or normally sited [4–7].

Since their identification by M. Urist, BMPs are the molecules most widely used in bone engineering due to their osteoinductive properties [8,9]. Among all the molecules that have been identified, BMP-2 and BMP-7 are the most studied and used in bone tissue engineering applications.

Following the initial successful pre-clinical studies, a large research effort led to the final approval of Infuse[®] Bone Graft (Medtronic, Dublin, Ireland) in the US and InductOS[®] (Wyeth, Madison, NJ, USA) in Europe. They were approved for use at spinal fusion, open tibial fractures, and tibia non-unions [10]. Clinical studies showed a significant decrease in fracture healing time, the secondary intervention rate, and hospital stay, while the cumulative complication rate was less than 0.5% [11].

Later clinical studies and systematic reviews after the wide use of clinical applications with recombinant human BMP-2 (rhBMP-2) highlighted safety concerns and adverse events not published initially, increasing the complication rate 10–50 times higher than what was initially reported [11]. Heterotopic ossification or bone resorption, excessive inflammation and edema causing dysphagia in cervical spine fusions and nerve root compression, and

wound-healing problems were some of the most frequently reported issues. According to the Food and Drug Administration's (FDA) Manufacturer and User Facility Device Experience (MAUDE), inflammation and ectopic ossification are responsible for 32% of the reported adverse incidents [12]. Concerns were also raised regarding the carcinogenic effects of BMP-2.

Attempts to diminish side effects have prominently focused on the study of various delivery systems. These systems must act as both carriers and scaffolds. Their role as carriers is to retain the growth factors at the site of interest for the desired, prolonged period of time and protect them from degradation while preserving bioactivity and permitting their controlled release. They must also act as scaffolds for cell migration, attachment, and differentiation [10,13,14].

Many aspects of bone tissue engineering using BMPs have been explored at a pre-clinical level. Studies of different concentrations and doses of BMP-2 or other growth factors, alternative delivery vehicles, separate solvents, and distinct animal models and protocols have been described, creating a large heterogeneity of applications each with its own strengths and limitations. However, the ideal application and product have yet to be described in order to maximize efficacy and safety in bone tissue engineering using BMPs.

Surprisingly, all documented applications in the literature have demonstrated positive outcomes with significant bone formation. Extensive documentation exists regarding the presence of osteoblasts, osteocytes, or bone marrow cells as well as descriptions of the osteoid and bone's organic component. Nevertheless, there is minimal information on the HA crystals and mineral constituents in general. The significance of this omission becomes better understood when it is considered that these crystals constitute almost 70% of the bone's net weight [15].

The aim of this review is to describe the different types of materials used in bone engineering applications in vivo and to present the evaluating techniques used to report their success, highlighting the absence of information on HA crystals that form the inorganic component of the bone.

2. HA Is Not the Only Calcium Phosphate (CaP) Crystal

Bone tissue is the main storage of calcium and phosphorus for the human body, with these elements predominantly existing in the form of calcium phosphate minerals, consisting of approximately 70% of the bone mass. Calcium phosphates belong to a large family of minerals that contain calcium ions (Ca^{2+}), combined with phosphate anions (Table 1). Apart from being part of living organisms and tissues (bone, enamel, and dentin), CaP compounds are extremely important for medicine, agriculture, and the food industry. They have been used as bone substitutes in hard tissue engineering and bone cement and as fertilizers, toothpaste and mouth hygiene products, and food additives [1,16].

Table 1. Calcium Phosphates (CaP) [1,16].

Orthophosphates (materials that contain Ca^{2+} combined with PO_4^{3-})
Tricalcium Phosphate— $\text{Ca}_3(\text{PO}_4)_2$
Octacalcium Phosphate— $\text{Ca}_8\text{H}_2(\text{PO}_4)_6 \cdot 5\text{H}_2\text{O}$
Amorphous Calcium Phosphate (ACP)
Di- and monohydrogen phosphates (materials that contain Ca^{2+} combined with HPO_4^{2-} or H_2PO_4^-)
Monocalcium phosphate— $\text{Ca}(\text{H}_2\text{PO}_4)_2$
Dicalcium phosphate— CaHPO_4 (monetite) or $\text{CaHPO}_4(\text{H}_2\text{O})_2$ (brushite)
Polyphosphates
Dicalcium Diphosphate— $\text{Ca}_2\text{P}_2\text{O}_7$
Calcium Triphosphate— $\text{Ca}_5(\text{P}_3\text{O}_{10})_2$
Apatites (materials that include other anions in addition to phosphate)
Hydroxyapatite— $\text{Ca}_{10}(\text{PO}_4)_6(\text{OH})_2$
Oxyapatite

Orthophosphates are one of the main categories of CaP. They characteristically include the group PO_4^{3-} . Tricalcium phosphate, octacalcium phosphate, and amorphous calcium phosphate (ACP) are included. Di- and monohydrogen phosphates have been used as well (HPO_4^{2-} or H_2PO_4^-), with representatives of monocalcium phosphate and dicalcium phosphate minerals (monetite and brushite). Polyphosphates include materials containing Ca^{2+} ions combined with di- or triphosphates ($\text{P}_2\text{O}_7^{4-}$ and $\text{P}_3\text{O}_{10}^{5-}$). Last but not least, apatites belong to the CaP family. They are materials that include other ions, in addition to phosphates. Hydroxyapatite ($\text{HA-Ca}_{10}(\text{PO}_4)_6(\text{OH})_2$) and oxyapatite are the best-known minerals.

CaPs are characterized by their calcium-to-phosphorus (Ca/P) ratio, which is unique for each material. HA has a Ca/P ratio of 1.67, whereas β -TCP has 1.5 [16,17]. Their properties, including mechanical properties, water solubility, and in vivo degradation, strongly depend on the Ca/P ratio [17]. Moreover, Boushell et al. described that ceramics with higher Ca/P ratios showed increased chondrocyte proliferation with early onset of ALP activity and mineralization [18].

Regarding the water solubility of CaP, as well as their degradation in vivo, HA is the least soluble CaP, showing the lowest degradation rate in vivo. Monocalcium phosphate has a greater degradation rate, followed by dicalcium and octacalcium phosphate. β -TCP shows low degradation in vivo, but its degradation rate is still higher than HA [16].

Hydroxyapatite (HA)

HA is the main mineral component in both cancellous and cortical mature bone. Bone HA is a carbonated HA (carbonate concentration varies between 2–9%) with a predominantly hexagonal crystal structure [19,20]. They are the smallest biogenic crystals with a plate-like or needle-like shape. They have a length of 50–100nm, width of 30–50nm, and thickness of 2–6 nm [19–21]. HA is fragile and weak under tension and shear forces, while it shows substantial resistance to compression loads [22].

HA crystallites are either associated with the collagen fibrils (intrafibrillar minerals) or exist in the space between those fibrils (extrafibrillar minerals) [20,21]. These two mineral fractions have differences in properties, function, and structure.

Intrafibrillar minerals are located either between the layers of the collagen molecules at the overlap region or at the gap region, forming the mineralized collagen fibrils (MCFs). MCFs are the basic building unit of bone tissue, and they are responsible for its mechanical properties at the nanoscale [20,23]. HA crystals of MCFs have a periodic appearance that corresponds to the periodicity of the collagen fibrils (D-period). Regarding the collagen–minerals interactions, it is thought that ionic bonds are formed between the side-chain carboxyls of collagen and calcium ions of the crystals [20].

On the other hand, extrafibrillar minerals account for almost 75% of the total amount of bone minerals. They are longer and thicker than their intrafibrillar siblings [20]. Another highly important element of the space between the fibrils is non-collagenous acidic proteins due to their significance and role in the initiation of the mineralization process [20]. Mineralization starts at this space, and the first CaP mineral to be formed during either the intramembranous or endochondral ossification is ACP, which is later transformed into HA [24]. The surrounding chemical environment (factors affecting pH) and mechanical stimuli (compressive or tensile stress and fluid shear stress) determine the actual crystal growth speed, size, and morphology [24,25].

3. In Vivo Research in Bone Engineering: Do They Care about the Formation of the Right HA Crystals?

3.1. Scaffolds Used in Bone Engineering

Research efforts have extensively explored polymers, whether natural or synthetic, and ceramics, each presenting distinct advantages and drawbacks in the realm of bone tissue engineering. While polymers offer versatility and customizable properties, ceramics

boast high mechanical strength and biocompatibility. However, neither material alone perfectly addresses all requirements for optimal bone regeneration.

In response to this challenge, composite scaffolds have emerged as a compelling solution. These scaffolds aim to harness the strengths of both polymers and inorganic materials, theoretically providing a balanced delivery system with enhanced protein-release capabilities. By integrating the unique characteristics of each component, composite scaffolds hold promise in overcoming the limitations associated with individual materials, paving the way for improved outcomes in bone tissue engineering.

Meanwhile, advancements in nanotechnology have opened new avenues for enhancing bone regeneration. Nanoscale modifications of implants offer an environment conducive to bone formation, leveraging the unique properties of nanomaterials to promote cellular interactions and tissue regeneration. As such, nanotechnology stands poised to play a pivotal role in driving innovation and progress in the field of bone engineering.

The following paragraphs provide an in-depth exploration of these materials and their wide-ranging applications in bone tissue engineering, complemented by individual tables (Tables S1–S5) to enhance clarity and understanding.

3.1.1. Polymers

Polymeric scaffolds are, in general, the most commonly used materials in bone tissue engineering applications. Their biocompatibility and biodegradability, as well as the ease of fabrication of different shapes and sizes, are the principal reasons for that. Important physiochemical parameters, such as porosity, pore size, solubility, and mechanical properties, can be controlled, improving the final scaffold.

1. Natural Polymers

The first materials used in tissue engineering were for the fabrication of natural polymeric implants. These consist of extracellular materials like proteins (collagen, gelatin, and fibrin) or polysaccharides (chitosan and alginate) (Table S1). Low cytotoxicity and favorable degradation products facilitated the rise in interest. In contrast, poor mechanical properties and rapid degradation raised concerns.

Collagen and Gelatine

Collagen is most commonly used in bone engineering. It is the most abundant matrix protein. A vast variety of collagen formulations have been used in preclinical studies in the literature, including gels, absorbable sponges (ACS), fibrils, the demineralized bone matrix (DBM), strips, membranes, and composites. The most used formulation is that of ACS.

Industrially manufactured sponges are a common practice in most recent studies. Helistat® (Integra) is the most frequent in bone engineering applications with BMPs. It consists of collagen derived from the bovine Achilles tendon. It has been cross-linked with formaldehyde and sterilized with ethylene oxide. Helistat® is clinically approved as a hemostatic sponge. It is used in surgical procedures as an adjunct to hemostasis. Uludag et al., in their series of studies, used, among other carriers, Helistat® sponges [26,27]. They used modified versions of rhBMP-2 and rhBMP-4 in various doses to assess osteoinduction. Carriers were allowed to soak within the growth factor solution for 10–30 minutes before being implanted subcutaneously in the thoracic region of Long Evans rats.

Loading time (or soaking time) varies in the literature from five minutes to one hour. Huang et al. additionally stored the implants overnight at 4 °C after soaking for 60 min at room temperature [28]. Loading time affects protein incorporation into the collagenous matrix. A slight increase in incorporation is noted by extending the soaking time. Denser matrices can also increase the binding of protein to ACS [29,30].

The solution used was not mentioned in most applications. Its importance has been highlighted in the literature. BMP-2 binding to ACS is highly affected by the pH and ion concentration of the protein's solution. Binding is negligible at pH 3–4 and increases significantly at pH 6–7 [29,30]. In those few that included this important information, it was either a phosphate buffer solution (PBS) [31] or an Infuse® solution [32,33].

Kato et al. also used 6 mm disks of Helistat[®], loaded with increasing rhBMP-2 doses (0, 1, 2, 5, 10, and 20 µg). ACS was lyophilized after BMP loading in order to show a dose-dependent reaction in bone formation at three weeks post-subcutaneous implantation on SPC mice [34]. Chen et al. manufactured a 10% *w/v* collagen sponge lyophilized pre- and post-incubation with BMP-2 solution, providing the final implant with a favorable burst of initial release and a sustained release profile [35].

Apart from Helistat[®], other industrially manufactured collagen implants have been used in similar applications. These include sponges (Mighty[®], Teruplug[®], and CollaTape[®]) and membranes (Hypro-Sorb[®]) [36–40].

Collagen matrices are versatile. Their manufacture includes several steps. Freeze drying is the most advantageous procedure to produce the necessary porous structure. Cross-linking affects the chemical and physical properties of the material and improves its mechanical properties and degradation ratio [29]. Chemical cross-linking is used for all industrially manufactured implants. Glutaraldehyde is the most common agent. Dehydrothermal treatment (heating under vacuum) or enzymatical cross-linking are alternative options [35,41]. The use of non-cross-linked scaffolds has rarely been described.

Sterilization is a necessary condition for every medical application, including laboratory animal surgery, although most authors do not mention the sterility status of their implants. Ethylene oxide (EtO) and γ -irradiation are processes widely used for sensitive medical devices like proteins and scaffolds, including collagen and natural polymers [32,42]. As with cross-linking, sterilization modalities have an impact on the microstructure of the implants, affecting their physico-chemical properties and, as a consequence, protein retention [26].

Kim et al. described a thought-provoking finding. They used 8 mm disks from the collagen membrane Collatape[®], which were loaded for 5 min with a solution of 5 µg of rhBMP-2 and then placed subcutaneously on Sprague–Dawley rats. Two weeks later, new bone was evident at the periphery of the implants, whereas this was resolved at eight weeks [40]. Absorption of the initially evident ectopic bone was also described by Saito et al., following the suffusion of collagen gel with 3 µg of rhBMP-2. No details regarding the implant used or the process of BMP loading were provided. Bone-like tissue was present three weeks post-implantation intra-muscularly into the calf pouches of Wistar rats, but this had disappeared at seven weeks [43].

DBM is derived from cancellous or cortico-cancellous bone through the removal of the mineral component using an acidic solution. It still contains structural (mainly type I collagen) and signaling proteins. It can be used as an alternative to an autologous bone graft and there are numerous commercially available products [44]. Additionally, it has been used in many bone tissue engineering applications. Tsiridis et al. prepared DBM from Wistar rat long bones and used it in combination with 2 µg of BMP-7 in an ectopic model, achieving superior osteogenesis compared to DBM alone or fresh frozen allograft (FFA) [45].

Gelatin is a natural polymer that is also commonly used in medical applications, including bone engineering. Gelatin is derived from collagen, but it has certain advantages. It is water soluble in neutral conditions and can form poly-ion complexes with growth factors and proteins. As it is a denatured derivative of collagen, it causes a weaker immune response [46].

Gelatin scaffolds are typically cross-linked to improve properties and degradation and are sterilized with EtO or γ -irradiation [47,48]. Both Yamamoto et al. and Takahashi et al. used gelatin scaffolds cross-linked with glutaraldehyde as a control group, showing more bone formation and ALP activity at four weeks than collagen and composite materials, respectively [42,49].

Polysaccharides and More Natural Polymers

Alginate is a polysaccharide of natural origin, which is particularly attractive for bone and cartilage tissue engineering applications. Saito et al. presented their fascinating work with a 20-mer peptide derived from the knuckle of BMP-2 linked or mixed with a cova-

lently cross-linked sterile alginate scaffold in the form of hydrogels or sponges [43,50–52]. Alginate hydrogels have also been used in addition to bone marrow stromal cells (BMSCs) to promote ectopic bone formation in mice with a minimal dose of 200 ng of rhBMP-2 [53]. Alginates can be further modified to improve their structure, properties, and cell affinity. In addition to lyophilization and cross-linking, this can happen through mixing with other materials, chemical surface modifications, or the immobilization of ligands like proteins and binding sequences, such as arginine-glycine-aspartic acid (RGD) [54–57].

Chitosan, a polysaccharide derived from chitin, has also been utilized in various forms, like hydrogels, meshes, composites, and derivatives. Luca et al. showed ectopic bone formation (both woven and trabecular) at three weeks following quadriceps injection of 0.2 mL of hydrogel containing a high dose (150 µg) of rhBMP-2 [58]. Chitosan is mainly used in combination with other materials or modified to improve bioactive molecule retention and release, as well as cell proliferation and adhesion and, therefore, final outcomes [10,14,59]. Bakopoulou et al. developed a chitosan–gelatin sponge, freeze-dried and cross-linked with glutaraldehyde, which was incubated with BMP-2 for 24 h [60]. Similarly, Park et al. manufactured injectable chitosan–alginate gel loaded with mesenchymal stem cells (MSCs) and a low dose (2 µg) of rhBMP-2 [61].

Hyaluronate is the third most common polysaccharide used in bone engineering. It has been used in various applications, such as hydrogels or sponges, as injectable or solid materials [10,14,62]. Commercially available gels Heprasil® and Glycosil® were used as rhBMP-2 vehicles by Bhakta et al. in a rat ectopic model [63,64]. They are hyaluronan-based hydrogels with or without heparin accordingly. Merogel® is a commercially available hyaluronan sponge, which was used in a similar way as collagen sponges and showed dose-dependent defect healing and bridging 8 weeks post-operation, with both rhBMP-2 and rhBMP-4 [65].

The introduction of functional groups and cell adhesion molecules led to modified hyaluronate derivatives. Such a derivative supplemented with collagen type I fibrils or fibronectin was manufactured by Bulpitt and Aeschlimann. They were freeze-dried, mixed with rhBMP-2, and then cross-linked with various low- or high-molecular-weight cross-linking agents [62].

In a simpler application, hyaluronate gel was mixed with a high dose of rhBMP-2 (200 µg) and was injected at the tibial defect site of rabbits showing 100% union [66]. The combination of a low dose of rhBMP-2 (0.8 µg) and MSCs on an acrylated hyaluronic acid gel showed a synergic effect on healing calvarian defects in rats with thicker and denser bone formation [67].

Dextran has been used as a protein carrier as well, as it is highly biocompatible and water-soluble. Functionalized dextran (FD)-derived hydrogels, sterilized by UV light and cross-linked with sodium trimetaphosphate, have been used successfully in a rat ectopic model by Maire et al. [68].

Fibrin and fibrin-related products are widely used as a wound sealant and for achieving hemostasis. Fibrin is a protein involved in blood clotting and wound healing and acts as a matrix in injured tissue. Fibrin matrices, mixed with 10 µg rhBMP-2 pre-solidification, showed similar bone formation to Infuse® collagen sponges at eight weeks in a segmental femoral defect on a rat model [69]. Similarly, fibrin glue blocks with 10 µg rhBMP-2 showed a similar amount of bone regeneration in segmental fibular defects with autoclaved autologous bone [37]. Tisseel®, a commercially available fibrin–fibronectin sealing system, with the addition of rhBMP-4, displayed the bridging of calvarian defects both at two and eight weeks, whereas trabecular bone was evident ectopically twelve weeks post-subcutaneous injection of gels of platelet-enriched fibrin glue with BMSCs and 2 µg of rhBMP-2 [70,71].

Silk proteins demonstrate favorable characteristics for bone engineering applications. They are degradable with high tensile strength and contain integrin binding motives. Their properties can be modified by cross-linking, and they can be used in combination with composite scaffolds [14,57,72]. Kirker-Head et al. fabricated disc-shaped silk scaffolds, which were autoclaved at 121 °C for 15 min and loaded with 2.5 µg of rhBMP-2 [73].

2. Synthetic Polymers

Synthetic polymers have attracted attention in bone engineering as safe alternatives to replace collagen and natural polymeric implants. They have been used predominantly in bone or calvarian defect models (Table S2). The risks of using xenogenic materials, like immune reactions and disease transmission, are eliminated. They are biodegradable and, as synthetic materials, their characteristics can be modified in a controlled manner to alter the drug delivery profile [10,14,43,74].

Poly-ε-caprolactone (PCL) is a bioresorbable material that has been used for years in tissue engineering. Patel et al. manufactured flower-shaped scaffolds, which were used in a mouse ectopic model with either conjugated or absorbed rhBP-2 (20 or 65 µg/mL). [75] The fact that it can be produced using 3D printing techniques means that the scheme, porosity, and degradation level can be altered or maintained as needed.

Porosity, at both macroscopic and microscopic levels, is a significant property of all scaffolds used in bone engineering. High porosity and large pore size are favorable for protein absorption, cell migration, capillary formation, and vascularization [72,76,77]. There is no precise recommendation for the optimal pore size. Scaffolds of various materials with pores sized between 50 and 600 µm have been described [52,78,79]. Initially, 100 µm was recommended as the minimum optimal pore size, whereas several studies have demonstrated more favorable results using scaffolds with pore sizes greater than 300 µm.

Poly-glycolic Acid (PGA), Poly-lactic Acid (PLA), and their copolymer, Poly-lactic-co-glycolic acid (PLGA), are all polymers of α-hydroxy esters. These materials were used for the first synthetic, absorbable sutures and are still used for that purpose. Additionally, they have attracted attention in bone tissue engineering applications [80]. Dexon® is a PGA mesh utilized in abdominal surgery, like hernia repair, abdominal partitioning, or packing in intra-abdominal bleeding. Uludag et al. included, among other scaffold materials, this industrially manufactured mesh in their experiments, measuring the osteoinductive potential of increasing doses of rhBMP-2, rhBMP-4, and succinylated rhBMP-2 [27].

3D-printed PLA scaffolds with a porosity of 60% and a mean pore size of 100 µm were functionalized with a thin coating layer of polydopamine (PD). This allowed Chen et al. to use low doses of rhBMP-2 (1 µg) in their ectopic model application [81]. A 5% PLLA solution was mixed with 60 µg of rhBMP-2, followed by freeze-drying, which resulted in disk scaffolds with a porosity of 90% and a mean pore size of 50–60 µm [79]. Jeon et al. fabricated heparin-conjugated (HP), porous PLGA scaffolds (pores sized 100–200 µm) in a rat ectopic model [82]. HP-PLGA scaffolds can degrade as slowly as 60 days in a phosphate buffer solution (PBS) at 37 °C and they can continue releasing rhBMP-2 for 14 days. These characteristics allowed Jeon et al. to use 1 µg of rhBMP-2, which resulted in extensive bone formation in the hind limbs of Wistar rats in eight weeks [82]. Hollinger et al. confirmed the bridging of a critical radius defect in rabbits when PLGA scaffolds were used in combination with either autologous blood or carboxymethyl cellulose (CMC). The results showed dose-dependent results [83].

Polyethylene Glycol (PEG) is a hydrophobic polyether, commonly used in tissue engineering and drug delivery due to its excellent biocompatibility. Lutolf et al. used cross-linked PEG-based hydrogels in a calvarian defect model. First, 5 µg of rhBMP-2 was incorporated into the scaffolds, non-covalently, during the cross-linking process, showing similar bridging and bone healing to Helistat®-treated defects with the same amount of rhBMP-2 [84,85]. TG-crosslinked PEG hydrogels of various stiffnesses were used by Vallmajo-Martin et al. to heal an 8mm calvarian defect. RGD motifs were not found to improve the final outcome [86].

Poly-Lactic Acid-Dioxanone-Poly-Ethylene Glycol (PLA-DX-PEG) is a tri-block copolymer that has been tested for successful rhBMP-2 delivery in a variety of animal models. Kato et al. confirmed a dose-dependent reaction in a mouse ectopic model, with complete resorption of the polymer [34]. Suzuki et al. used a scaffold with a PLA/DX/PEG ratio of 5:1:3. Scaffolds were used to carry 5 µg of rhBMP-2 with or without antibiotics, showing no impact of the antibiotics on material osteoinduction [87].

3. Overall

In conclusion, polymeric scaffolds, whether derived from natural sources or synthetically engineered, offer versatility in various applications. Significant advances have been made in the manufacturing process over the past years. The magnitude of porosity, cross-linking, and sterilization has been thoroughly studied, and scaffolds have been optimized accordingly, leading to FDA-approved products. Nevertheless, preclinical studies have often failed to describe the presence of all elements that compose bone tissue. More specifically, while significant emphasis has been placed on reporting the presence and behavior of cells and extracellular matrix, little attention has been paid to the equally vital inorganic component crystals that form an integral part of bone structure. This oversight underscores the need for a more holistic approach to scaffold design and characterization, ensuring that all facets of bone tissue composition and functionality are adequately addressed for optimal performance and clinical efficacy.

3.1.2. Ceramics

Ceramics is a large category of bioactive, inorganic materials used as bone graft substitutes and in bone tissue engineering applications (Table S3). They have the advantage of superior mechanical strength compared to polymers, similar to that of the mineral part of the bone [14,57,72,74]. Additionally, ceramic scaffolds can be optimized by the modification of their physical properties, porosity, degradation rate, biocompatibility, or solubility [74]. CaP materials belong to this category.

Hydroxyapatite (HA) has been used in various formulations in bone tissue engineering, including powder, particles, blocks, and disks [10,88]. There has been significant debate regarding the optimal characteristics of HA scaffolds. The usual manufacturing technique is sintering HA powder into the final implant at high temperatures [77,78,89]. This technique creates porous implants, which are generally considered more effective. It seems that pore sizes between 300 and 400 μm promote osteoinduction [78].

Murata et al. used porous particles of HA that were sintered to a scaffold with a porosity of 70% and a mean pore size of 150 μm . Specifically, 300 μg of partially purified BMP was mixed with the scaffold and scaffolds were implanted subcutaneously in an ectopic rat model [89]. HA porous scaffolds have been tested with a combination of low-dose rhBMP-2 (1 μg) and MSCs, and this has also proven successful in promoting de novo bone formation in an ectopic rat model [90].

Tricalcium phosphates (TCPs) are brittle materials with a slow degradation rate in vivo that have been studied thoroughly as BMP carriers [74,88]. Liang et al. used sintered porous β -TCP ceramics with a porosity of 42.3% and an average pore size of 300–400 μm immersed in a solution of 50 μg of rhBMP-2. Ceramics were lyophilized following immersion and then sterilized with ethylene oxide before implantation intramuscularly in mouse thigh muscle pockets [91].

Cerasorb[®] is a commercially available series of β -TCP products, like particles, pastes, or foam sponges. They are commonly used in dental surgery. Kim et al. used Cerasorb[®] particles loaded with 5 μg of rhBMP-2 in a rat ectopic model and compared it to Helistat[®] sponges soaked for five minutes in the same BMP solution. Both materials showed bone formation in two weeks post-implantation. β -TCP groups showed progression of bone formation at week 8, whereas in Helistat[®] groups, bone was not visible as had been resolved [40]. In contrast, Pang et al. found no difference in bone formation between the Cerasorb[®] sponge and Collatape[®], a commercially available collagen sponge. Both materials were loaded with 2.5 and 5 μg of rhBMP-4 for five minutes before implantation in a rat segmental defect model [39].

Ceramics have demonstrated their superiority in providing robust mechanical properties essential for specific applications. Porosity and manufacturing processes have again proven highly important. CaP scaffolds with a slow degradation rate have been commonly used. Despite that, the origin of calcium deposits and evidence of mineralization seen a

few weeks post-surgery was not meticulously checked, and it is not clear whether new HA crystals have been formed, raising questions about the efficacy of current practices.

3.1.3. Composites

Bioactive materials have been combined to create composite scaffolds that, theoretically, could combine the advantages of these materials (Table S4). Polymeric/ceramic materials have gained attention as they develop improved mechanical properties and biocompatibility with controlled biodegradation [14,74]. They are considered to mimic bone structure and approximate its properties [74].

1. Natural Polymers/Ceramics Composites

Natural polymers/ceramics are a common combination with collagen or gelatin, forming a composite with β -TCP or HA. Gelatin has been combined with different contents of β -TCP to form composites for rhBMP-2 delivery in vivo. Gelatin was cross-linked with glutaraldehyde at 4 °C for 12 h in the presence of β -TCP, followed by freeze drying of the final material [49,92–94]. The delivery of 17 μ g of rhBMP-2 in segmental defect models showed complete healing of the defect with no difference between composites and gelatin sponges [93,94]. In contrast, Takahashi et al., in a subcutaneous ectopic model, confirmed an inversely proportional relationship between the amount of β -TCP and osteoinduction, despite homogenous bone formation in all rhBMP-2 groups after 4 weeks [49]. It is highly interesting that similar findings were reported by Luca et al. using a chitosan/ β -TCP composite [58].

A composite implant of carboxymethylcellulose (CMC) with β -TCP particles (a mixture of 1:2) was used by Tsiridis et al. in a non-critical defect model [95]. A single-level, wedge-shaped osteotomy was created at the lateral aspect of the right distal tibial metaphysis of white New Zealand rabbits. The gap was either left unfilled or the composite implant was used. Next, 200 μ g of OP-1 was injected into the implant. Alternatively, daily subcutaneous injections of 10 or 40 mg/kg of the parathyroid hormone (PTH) were administered for 3 weeks. Interestingly, the use of OP-1 was related to superior bone healing, whereas systemic administration of PTH showed more global bone formation [95].

Susin et al. combined Helistat[®] sponges with Mastergraft[®], a biphasic ceramic of 15% Hydroxyapatite (HA) and 85% β -Tricalcium Phosphate (β -TCP), to create a composite material. They used the scaffold in a sinus augmentation model in Göttingen mini pigs. Loading scaffolds with 1.72 mg rhBMP-2 as per Infuse[®] BoneGraft instructions again showed lower bone formation in the composites than ACS alone at 8 weeks post-implantation [96]. Collagraft[®], a commercially available composite material that is a combination of purified Type I bovine dermal fibrillar collagen with 65% calcium hydroxyapatite and 35% TCP, was compared to MeroGel[®], a hyaluronian sponge in a defect model [97].

Collagen/HA composites have also been proven to promote bone healing in defect models. Specifically, 2 μ g of rhBMP-2 was mixed with collagen-HA slurry, followed by lyophilization and sterilization under UV light ($\lambda = 254$ nm) for 4 h. Final disk implants (diameter of 7 mm, average pore size of 100 μ m) were placed into calvarian defects showing, at 8 weeks, full healing with thick, mature bone, with a structure similar to native bone [98]. An extremely large amount of human BMP-4 (10 grams) was loaded in collagen/HA microspheres sized 600–700 μ m, showing evidence of active bone formation [99].

As mentioned previously, gelatin is one of the materials that has been studied extensively in the formation of composite scaffolds. Gelatin sponges containing different concentrations (0% wt, 50% wt, and 90% wt) of Magnesium Calcium Phosphate (MCP) were used in a rat defect model. Gelatin/MCP scaffolds were freeze-dried and dehydrothermally cross-linked. They were loaded with 2.5 μ g of rhBMP-2 before implantation in a cranial, rat defect model showing significant bone formation both at 3 and 12 weeks, especially for the 50% wt scaffold [100]. A biphasic ceramic powder of Calcium Sulphate (CaS)-HA (60–40%) was mixed with a 5% gelatin solution, followed by cross-linking with glutaraldehyde, to create a composite porous scaffold (30–110 μ m). When compared to Helistat[®] in an intra-

muscular ectopic model, it showed a higher mineralized volume with a dose-dependent reaction [101].

2. Synthetic Polymers/Ceramics Composites

Synthetic polymers are again alternative materials in the formulation of composite scaffolds. The addition of ceramics aimed to improve the plasticity and general properties of final implants. Kato et al. combined PLA-DX-PEG with various amounts of β -TCP and low doses of rhBMP-2 (2 and 5 μ g) in a mice ectopic model to show that the volume of new bone formation at three- and six-weeks post-implantation increased linearly with an increase in the β -TCP ratio of up to 66.7% and then decreased [102]. Similarly, Matsushita et al. used a composite material with 75% β -TCP and low (5 μ g) or high (20 μ g) rhBMP-2 doses in a defect rabbit model. As was expected, groups with higher doses of rhBMP-2 showed significantly thicker cortical bone formation at six weeks [103]. In the above-mentioned studies, a copolymer was mixed with β -TCP and rhBMP-2 solutions to form the final implant, but no further details were provided. In contrast, Yoneda et al. immersed β -TCP cylinders in PLA-PX-PEG and rhBMP-2 solution under vacuum for a few seconds, resulting in copolymer coated β -TCP implants. [104].

A similar technique was adopted to create a mixture of liquidized copolymer PLA-PEG with the rhBMP-2 solution. Kaito et al. dropped a mixture containing 5 or 20 μ g rhBMP-2 onto interconnected porous HA scaffolds and applied the final coated implant to a rabbit radius critical defect model [105]. On the other hand, Murakami et al. submerged a cylindrical pure titanium fiber mesh implant in a high-dose rhBMP-2 mixture (60 or 120 μ g), which was then applied to a rat humeral defect model. Porous HA scaffolds had an interconnectivity of 90%, while titanium implants had a porosity of 50% with 350-400 μ m average pore size [106].

Polymer Composites

In research on new osteoinductive materials, natural and synthetic polymers have also been combined to provide new scaffolds. PLGA is mostly used in such combinations in the literature. PLGA-coated gelatin sponges were manufactured using freeze-dried gelatin sponges, cross-linked with dry heating at 155 $^{\circ}$ C, which were submerged in an 8% PLGA solution, followed by lyophilization [105]. These composites have been evaluated in both a rat ectopic model and a rabbit defect model, with high doses of rhBMP-2 showing calcified areas with trabecular bone and defect bridging, respectively [107,108].

PLGA microspheres have been added to Oligo-PEG fumarate (OPF), phosphate modified (BP) and not, or CMC. AN OPF/PLGA microsphere composite was cross-linked using UV light 365 nm for 40 min. Furthermore, 2 μ g of rhBMP-2 was encapsulated either by entrapment in microspheres (for sustained release) or absorbed by the composite (for burst release) or combination. There was no difference in bone volume regardless of the BMP loading methods. On the other hand, phosphate modification resulted in substantial bone formation in both models at nine weeks [109].

Blood clots have also been used as an organic part of composite materials [110,111]. Irie et al. combined blood clots with PLA-PGA copolymer microspheres. Specifically, 20 μ g of rhBMP-2 was added to the composite, which was implanted subcutaneously into rats' thoraxes, resulting in bone matrix appearance by day 5 [111]. Lee et al. used blood clots and PLGA particles of different sizes (247 or 430 μ m), sterilized by ethylene oxide. They added various amounts of rhBMP-2 (0, 0.93, 3.1, or 9.3 μ g) in a rat segmental femoral defect model. The smaller the particle PLGA size and the larger the amount of rhBMP-2 was, the greater the torsional stiffness and strength of the newly formed bone [110].

Overall

Combining materials of different categories to create composite scaffolds could imitate bone characteristics. However, pairing varying ratios of each material seems to have a heterogenous effect on bone formation underscoring the complexity of such applications. Thus, the presence of both organic and inorganic elements of bone within these scaffolds

has to be confirmed to ensure their ability to accurately replicate the intricacies of natural bone structure and function.

3.1.4. Nanoparticles

Nanostructures can mimic specific bioenvironments by designing constructs with specific biochemical, mechanical, and electrical properties. Therefore, tissue can be engineered by employing these nanostructures for enhanced cell adhesion, growth, and differentiation (Table S5). Mesoporous silica nanoparticles (MSNs) are commonly used in the literature due to their advantages of amenable pore size, large surface area, and surface functionalization. MSNs with a mean diameter size of 130 nm (100–200 nm), with or without dexamethasone, were coated with chitosan gelfoam (chi-MSN) that was distributed in a BMP-2 solution for four hours [112]. In slightly different scaffolds, Zhou et al. covalently grafted 100 µg of a 20-mer BMP-2-derived (residues 73–92) synthetic peptide onto MSNs gelfoam (nanoparticle diameter of 255 nm), followed by the addition of a dexamethasone solution [113]. Both studies used a rodent ectopic model with evidence of calcium depositions and bone formation in all groups. The addition of dexamethasone improved the results in both applications [112,113].

Mohammadi et al. used electrospinning to create PLLA nanofibers (diameter of 541 nm) and deposited nanoHA (size of 70 nm) on their surface in an attempt to mimic the bone extracellular matrix (ECM). Additionally, they immobilized liposomal nanocarriers on the surface of their scaffolds, loaded with a BMP-2-derived synthetic 20-mer peptide, the same as previous studies described [114]. In another recent application, Li et al. manufactured a nanoscaffold using gelatin microspheres (GMS) and nanoHA, loaded with rhBMP-6 with a final concentration of 100 ng/mL. rhBMP-6 was encapsulated in GMS via adsorption and lyophilization [115].

PLGA nanospheres (size 300 nm), loaded with 5 µg of rhBMP-7, were immobilized on PLLA macroporous and nanofibrous PLLA disk scaffolds, previously sterilized with ethylene oxide [116]. Weng et al. created a 3D nanofiber aerogel using a PLGA–Collagen–Gelatin (PCG) composite and bioglass (BG) nanofibers. The final construct was freeze-dried and thermally cross-linked at 520 °C for 10 min [117].

Three-dimensional (3D)-printed scaffolds have attracted attention as they offer flexibility over certain characteristics, i.e., porosity, interconnectivity, and shape. Ceramic nanoparticles and synthetic polymers are the materials utilized. Chen et al. used HA nanoparticles to print scaffolds that were eventually loaded with BMP-2 or VEGF and were used to heal 15-mm calvarian defects in New Zealand rabbits [118]. Similarly, Helaehil et al. printed their scaffold using PCL and either 20% *w/w* HA or β-TCP [119].

3.2. Describing the Newly Formed Bone

As mentioned above, describing success in bone engineering applications is mainly based on histologic and radiographic examination of the samples.

3.2.1. Histologic Evaluation

Hematoxylin and eosin (H&E) staining is the standard histologic stain used in the literature. This dye combination stains nuclei blue or purple, whereas the extracellular matrix, collagen, cytoplasm, and other structures become various shades of pink [120]. Useful cellular details can be revealed as H&E can identify various cells and tissues by providing information on the morphology and structures of a tissue, as well as patterns and shapes of cells within this tissue [120,121]. Patel et al. used H&E staining to describe cells, vessels, the tissue matrix, and the general tissue morphology [75].

H&E is considered the “gold standard” stain in histology with the diagnosis of various pathologies (Figure 2). In bone tissue engineering applications, it is used to describe the presence of osteoblasts or osteoclasts. Harversian systems and bone marrow cells set the diagnosis of mature bone formation. Characteristically, Omura et al. described the foci of new immature bone with osteoblasts at the periphery of the sponges with rhBMP-2

two weeks following implantation, whereas, at four weeks, mature lamellar and trabecular bone with osteocytes and marrow cavities were present in treatment groups [41].

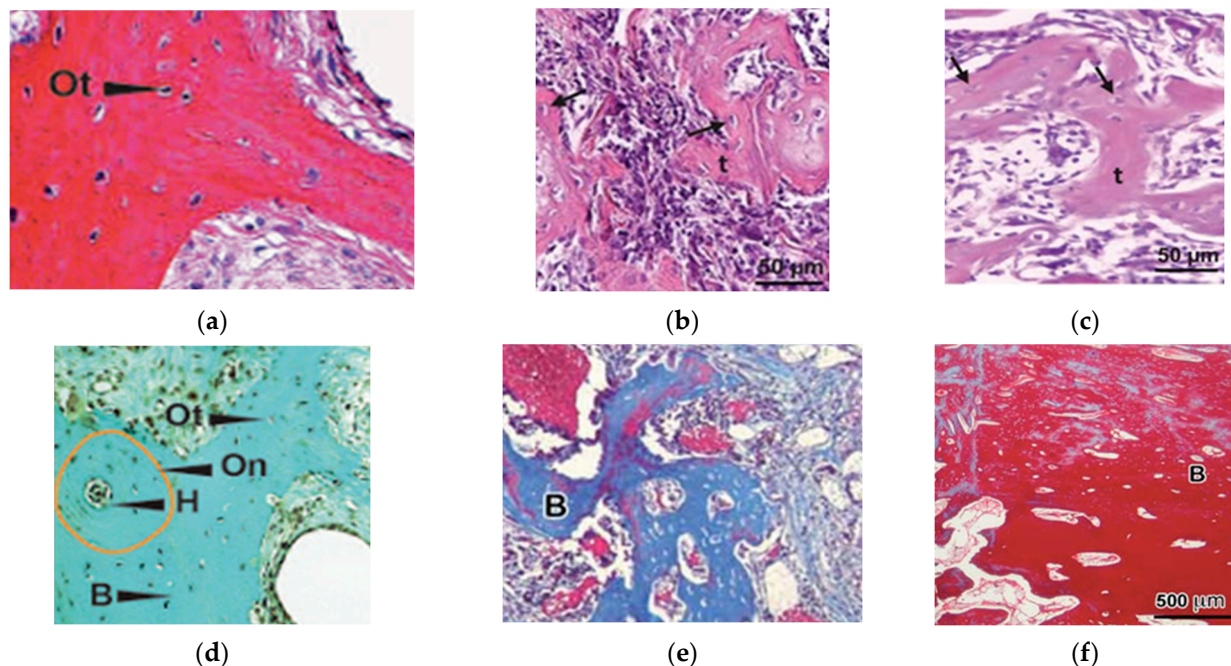


Figure 2. Histologic evaluation and bone tissue engineering: (a–c) H&E stain showing osteocytes characteristically entrapped within bone matrix; (e,f) Masson's trichrome of the structure of an osteon (d) and poorly (stained blue) and densely (stained red) mineralized bone. Adapted with permission from Ref. [58] 2010 Wiley Periodicals Inc., Hoboken, NJ, USA, [122] 2014 Landes Bioscience, Austin, TX, USA, [123] 2015 Wiley Periodicals Inc.

The Masson–Goldner trichrome and von Kossa staining have also commonly been used in the evaluation of bone engineering applications. They have been used in addition to H&E staining to evaluate mineralization. Other stains (i.e., Alcian blue, Safranin-O, Movat's pentachrome, Toluidine blue, and TRAP) are used less frequently [28,54,122,124].

The Masson–Goldner trichrome allows tissue identification through different coloring and morphological identification (Figure 2). It is used to differentiate collagen, fibrous tissue, and mineralized and unmineralized matrices [122,124,125]. The modified Masson trichrome can offer a clear distinction between connective tissue and bone matrix [122]. Luca et al. described a semi-quantitative evaluation method based on the Masson trichrome. The features they evaluated were carrier persistence, muscle atrophy, types and amounts of inflammatory cells, the presence of fibrous tissue, bone maturation and mineralization, and, finally, bone marrow formation [125].

The Von Kossa stain was predominantly developed and used for the detection and quantification of mineral deposits in tissues [41,42,82,126]. Krishnan et al. confirmed mineralization of the femoral defect region and the surrounding heterotopic nodules in a rat model [54]. Chang et al. stained their samples resulting from a rat ectopic model using H&E, Masson trichrome, and von Kossa stains to evaluate collagen and calcium deposition [79].

Histologic evaluation in bone engineering applications has to be viewed with skepticism. The reason for that is the application of decalcification (or demineralization) of the samples, before or after paraffin embedment. CaP minerals consist of 70% of the bone mass. Decalcification is the process of removing calcium salts from mineralized tissue. It is performed routinely to soften the tissue for subsequent segmentation and ultramicrotomy. It is a necessary process when evaluating hard and dense samples, like mature bone

and teeth. However, it might be unnecessary or even undesired in certain circumstances. Developmental studies or bone sarcoma evaluations are such examples [127,128].

The decalcification of samples in bone engineering applications, especially in ectopic bone models or when ceramic scaffolds are used, should be a major concern as well. Decalcification is common when H&E is the only stain used [7,34,40,45,102,112], whereas researchers tend not to use it when the von Kossa stain is selected [42,79,82,116]. Unfortunately, Omura et al. decalcified histologic sections that were stained with H&E and von Kossa [40]. Bhakta et al. used decalcified sections with H&E stain but undecalcified ones for the von Kossa stain in a rat ectopic model [64]. Another practice described is the decalcification of samples following the radiographic evaluation of mineralized volume [125].

3.2.2. Radiologic Evaluation

Radiology serves to complete the evaluation of the newly formed tissue and confirm the presence of bone. It is mostly used to evaluate the mineral compound of the bone. Micro-computed tomography (Micro-CT) is the most commonly used modality (Figure 3). Measuring radiodensity could theoretically not only identify bone tissue but also measure its volume. Concern has to be raised, however, for the accuracy of this method. The reason for that is the threshold in radiodensity set for detecting bone. Fat et al., in their *in vitro* study, described the inner cortical line at proximal humeri to be between 500 and 900 Hounsfield Units (HU) with a mean value of 700 HU. A value of 300 HU was considered to be cancellous bone, whereas the outer cortical line was at 1100 HU [129]. Similar findings were recorded in the literature [130,131]. Despite that, Bhakta et al. used threshold values between -315 and 543 HU for the quantification of bone in their bone tissue application, while Chen et al. used 0–4000 HU [35,64]. Raina used a more scientifically proper way as they calibrated their measurements against HA phantoms of known densities. Interestingly, they set their threshold to 4600 HU [101].

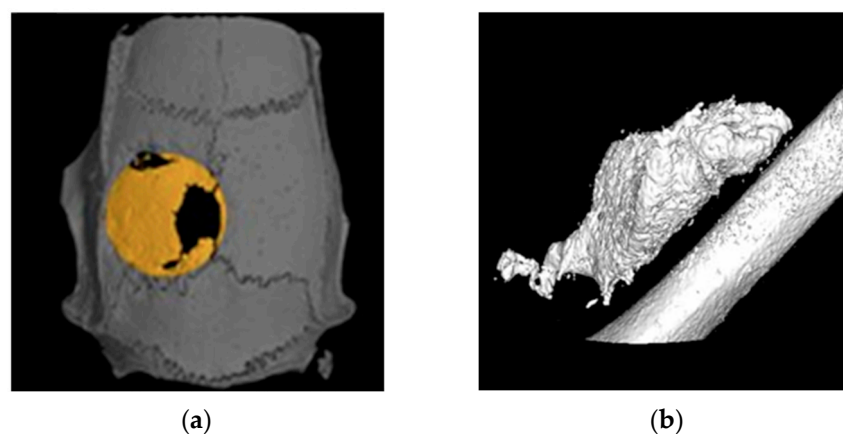


Figure 3. Micro-CT 3D reconstruction images showing (a) almost complete filling of the cranial defect 4 weeks post implantation; (b) ectopic bone formation at 3 weeks, modified from [35,58]. Adapted with permission from Ref. [58], 2010 Wiley Periodicals Inc.

In trying to quantify the newly formed bone and measure its volume for comparison purposes, mineral content (BMC) was measured. This was achieved using peripheral quantitative computed tomography (pQCT). Saito et al. calculated areas denser than 250 mg/cm^3 [43]. Dual-energy X-ray absorptiometry (DEXA) is traditionally used for measuring BMC, so it plays a role in bone engineering [34,87].

3.2.3. Functional Evaluation

Immunohistochemistry (IHC) has also been used to confirm new bone formation. Histology provides morphologic evaluation, but, in contrast, IHC reveals the functional

anatomy and can recognize specific agents and biomarkers with the use of antibodies against them [132]. Alkaline phosphatase (ALP), osteocalcin (OC), osteopontin (OP), and osteonectin (ON) are commonly used [35,40,123].

3.3. Characterizing HA Crystals

The common characteristic of all the previously described techniques is the fact that they are unable to evaluate and describe crystals and their structure. Light microscopy and its limit of resolution make it impossible to detect CaP crystals. Even mineral-specific stains, like von Kossa or Alizarin S, fail to differentiate apatite minerals and hydroxyapatite from other types of CaP crystallites [133,134].

Electron microscopy with its greater resolution and higher magnification could overcome the limitations of conventional optical microscopy. Scanning Electron Microscopy (SEM) and Transmission Electron Microscopy (TEM) are the two most common types of electron microscopy used in research. Both types work with a focused beam of electrons towards a sample and the image is created by the interactions of that beam and the sample. SEM scans the surface of the sample and creates an image detecting the reflected electrons, while TEM uses transmitted electrons that create the image by passing through a thin sample. SEM provides information on the surface of the sample at macro- and micro-scales, whereas TEM provides details of the inner structure of the sample at the nanoscale [135,136].

In addition to histologic staining (H&E and Masson's trichrome), Bakopoulou et al. used SEM examination combined with energy-dispersive X-ray spectroscopy (SEM-EDX) for both in vitro and in vivo studies. SEM showed images of mineralized particles with a minimum size of 50 nm. EDX evaluation showed a calcium-to-phosphorus ratio (Ca:P) of 1.4 for in vitro scaffolds and close to 1 after in vivo implantation. The latter is not that close to the ratio of the biological hydroxyapatite [60].

An imaging mode of TEM, called high-resolution TEM (HRTEM), allows the imaging of the atomic structure of various samples. Regarding biomaterials, HRTEM is considered a powerful tool that allows the study of their crystallographic structure at an atomic scale. Selected Area Electron Diffraction (SAED) is another technique performed using TEM. SAED can be used to describe crystal orientation and composition, measure lattice constants, and determine any defects (Figure 4). Xue et al. used both HRTEM and SAED for the characterization of intrafibrillar HA nanocrystals of MCFs in vitro [137].

Also, Atomic Force Microscopy (AFM) is a type of Scanning Probe Microscopy (SPM) that demonstrates resolution down to atoms, at fractions of a nanometer. It is an extremely powerful research tool, but its high cost and training needs have prevented it from becoming widely used [134].

Spectroscopic methods rely on the recognition of substances through spectra emitted or absorbed by them and comparing them with known spectra of specific compounds. Fourier-Transform Infrared Spectroscopy (FTIR) has been applied to characterize various tissues and scaffolds. Since the HA absorption FTIR spectrum has been reported, this technique could theoretically be used for determining the existence of HA crystals in the final samples of bone engineering applications [134,138].

Last, but not least, X-ray diffraction analysis (XRD) is a rapid analytical non-destructive technique used to determine the crystallographic structure of a sample or material. It also provides detailed information about the chemical composition and physical properties of this material. The generated X-rays are directed to the material, where their interaction produces a diffracted ray, which is scattered in various directions. This ray is then detected and processed. Each phase of the material produces a unique diffraction pattern due to its specific chemistry and atomic arrangement [134,139]. The qualitative phase analysis of the XRD pattern is compared with standard crystallographic databases and this leads to the phase identification of the material [138–140].

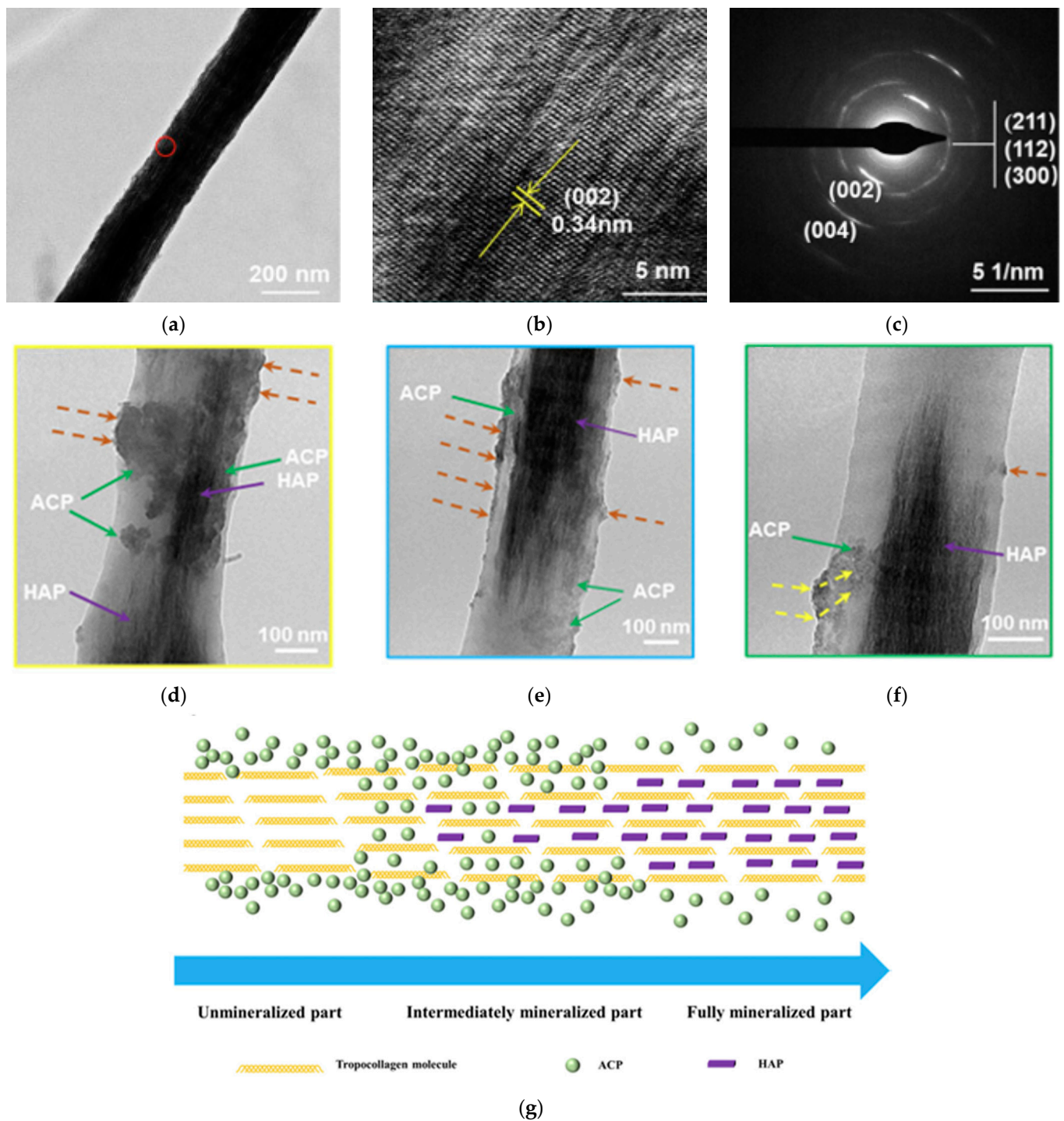


Figure 4. Orientation and composition of intrafibrillar HA nanocrystals: (a) TEM image; (b) HRTEM; (c) SAED; (d–f) ACPs infiltrating the collagen fibril and transforming into HA; (g) schematic presentation of the process of formation of mineralized collagen fibrils, modified from [137].

The usefulness of XRD in the identification of HA crystals is undeniable. As mentioned before, SEM-EDX examination of *in vivo* samples by Bakopoulou et al. showed a Ca:P ratio not close to that of biological HA. Despite that, XRD analysis performed on those samples confirmed the apatite nature of the newly formed mineralized tissues as HA's characteristic diffractogram was evident [60].

Saito et al., in their studies of a peptide derived from BMP-2, used XRD analysis to confirm that the pattern found in their sample when the peptide was added was identical to that of the rat's tibia and the major peaks were those of HA [43,50].

4. Conclusions

Since the identification of BMPs, great progress has been achieved in the field of bone tissue engineering. However, the challenge of designing a structure that can effectively mimic the mechanical, structural, and osteoinductive properties of the bone extracellular matrix remains [141]. The present review collocates the various materials and delivery systems that have been used, all with significant successful outcomes.

Polymers, natural or synthetic, and ceramics have been studied, each with its own advantages and disadvantages. Composite scaffolds are becoming attractive, as, theoretically, they can combine properties of both polymers and inorganic materials into a more balanced delivery system, offering more advantageous protein release. The nanoscale modification of implants offers a more favorable environment for bone formation, and nanotechnology applications have their role in the field of bone engineering.

Reporting the final outcome and describing the successful and more or less sophisticated applications rely on histologic and radiographic evaluation. The “gold standard” H&E offers morphological identification, as does Masson's trichrome. The Von Kossa stain offers recognition of mineralization and CaP deposits. Of great concern is the fact that decalcification still remains part of the process and the protocol until the final staining, with a potential impact on the results. Radiographic modalities attempt to measure the volume of the newly formed mineralized tissue.

It is at least thought-provoking that evaluating techniques used in the vast majority of bone engineering applications are unable to identify the presence of HA crystals. Research in the literature describes newly formed bone tissue, but cannot assess and prove the existence of the mineral that constitutes 70% of the bone mass.

In clinical cases, when bone pathology is studied, perhaps it is not necessary to identify HA crystals. Conventional microscopy with standard stains and radiology offers the required information. However, in research applications, especially when de novo bone formation in an ectopic, non-bone environment is studied, it is important to describe all organic and inorganic elements that form the bone tissue. Moreover, when using ceramic or composite scaffolds of CaP materials, it is a prerequisite to corroborate scaffold degradation and the formation of new HA crystals.

Incorporating advanced techniques such as Electron microscopy, spectrographic techniques, and XRD analysis into the evaluation process can provide deeper insights. By leveraging their strengths and understanding their limitations, researchers can effectively choose the most appropriate method for their specific research goals. This approach ensures robust and comprehensive evaluation of bone tissue engineering outcomes, ultimately advancing the understanding of bone regeneration and contributing to the development of more effective treatments and therapies.

Supplementary Materials: The following supporting information can be downloaded at: <https://www.mdpi.com/article/10.3390/cryst14050448/s1>, Table S1: Natural polymers; Table S2: Synthetic polymers; Table S3: Ceramics; Table S4: Composites; Table S5: Nanoparticles–Microparticles. Refs. [142–146] are cited in Supplementary Materials.

Author Contributions: Conceptualization, A.-N.T. and A.A.; methodology, A.-N.T.; validation, A.-N.T., C.K. and N.K.; investigation, A.-N.T., C.K. and N.K.; writing—original draft preparation, A.-N.T., C.K. and N.K.; writing—review and editing, A.-N.T., C.K., N.K., M.K., M.P., G.K., A.C., T.C.-P., A.A. and E.T.; supervision, G.K., A.C., T.C.-P., A.A. and E.T.; project administration, A.A. and E.T. All authors have read and agreed to the published version of the manuscript.

Funding: This research received no external funding.

Data Availability Statement: No new data were created or analyzed in this study. Data sharing is not applicable to this article.

Conflicts of Interest: The authors declare no conflicts of interest.

References

1. Sadat-Shojai, M.; Khorasani, M.T.; Dinpanah-Khoshdargi, E.; Jamshidi, A. Synthesis Methods for Nanosized Hydroxyapatite with Diverse Structures. *Acta Biomater.* **2013**, *9*, 7591–7621. [\[CrossRef\]](#) [\[PubMed\]](#)
2. Fraile-martínez, O.; García-montero, C.; Coca, A.; Álvarez-mon, M.A.; Monserrat, J.; Gómez-lahoz, A.M.; Coca, S.; Álvarez-mon, M.; Acero, J.; Bujan, J.; et al. Applications of Polymeric Composites in Bone Tissue Engineering and Jawbone Regeneration. *Polymers* **2021**, *13*, 3429. [\[CrossRef\]](#) [\[PubMed\]](#)
3. Einhorn, T.A. Enhancement of Fracture Healing. *Instr. Course Lect.* **1996**, *45*, 401–416. [\[CrossRef\]](#) [\[PubMed\]](#)
4. Pountos, I.; Panteli, M.; Lampropoulos, A.; Jones, E.; Calori, G.M.; Giannoudis, P.V. The Role of Peptides in Bone Healing and Regeneration: A Systematic Review. *BMC Med.* **2016**, *14*, 103. [\[CrossRef\]](#) [\[PubMed\]](#)
5. Westerhuis, R.J.; Van Bezooijen, R.L.; Kloen, P. Use of Bone Morphogenetic Proteins in Traumatology. *Injury* **2005**, *36*, 1405–1412. [\[CrossRef\]](#) [\[PubMed\]](#)
6. Shah, P.; Keppler, L.; Rutkowski, J. Bone Morphogenic Protein: An Elixir for Bone Grafting—A Review. *J. Oral Implantol.* **2012**, *38*, 767–778. [\[CrossRef\]](#) [\[PubMed\]](#)
7. Visser, R.; Rico-Llanos, G.A.; Pulkkinen, H.; Becerra, J. Peptides for Bone Tissue Engineering. *J. Control. Release* **2016**, *244*, 122–135. [\[CrossRef\]](#) [\[PubMed\]](#)
8. Urist, M.R. Bone: Formation by Autoinduction. *Science* **1965**, *150*, 893–899. [\[CrossRef\]](#) [\[PubMed\]](#)
9. Grgurevic, L.; Pecina, M.; Vukicevic, S. Marshall R. Urist and the Discovery of Bone Morphogenetic Proteins. *Int. Orthop.* **2017**, *41*, 1065–1069. [\[CrossRef\]](#)
10. Bessa, P.C.; Casal, M.; Reis, R.L. Bone Morphogenetic Proteins in Tissue Engineering: The Road from Laboratory to Clinic, Part II (BMP Delivery). *J. Tissue Eng. Regen. Med.* **2008**, *2*, 81–96. [\[CrossRef\]](#)
11. James, A.W.; LaChaud, G.; Shen, J.; Asatrian, G.; Nguyen, V.; Zhang, X.; Ting, K.; Soo, C. A Review of the Clinical Side Effects of Bone Morphogenetic Protein-2. *Tissue Eng. Part B Rev.* **2016**, *22*, 284–297. [\[CrossRef\]](#) [\[PubMed\]](#)
12. Nguyen, V.; Meyers, C.A.; Yan, N.; Agarwal, S.; Levi, B.; James, A.W. BMP-2-Induced Bone Formation and Neural Inflammation. *J. Orthop.* **2017**, *14*, 252–256. [\[CrossRef\]](#) [\[PubMed\]](#)
13. Poon, B.; Kha, T.; Tran, S.; Dass, C.R. Bone Morphogenetic Protein-2 and Bone Therapy: Successes and Pitfalls. *J. Pharm. Pharmacol.* **2016**, *68*, 139–147. [\[CrossRef\]](#) [\[PubMed\]](#)
14. Agarwal, R.; García, A.J. Biomaterial Strategies for Engineering Implants for Enhanced Osseointegration and Bone Repair. *Adv. Drug Deliv. Rev.* **2015**, *94*, 53–62. [\[CrossRef\]](#) [\[PubMed\]](#)
15. Fuchs, R.K.; Warden, S.J.; Turner, C.H. Bone Anatomy, Physiology and Adaptation to Mechanical Loading. In *Bone Repair Biomaterials*; Planell, J.A., Best, S.M., Eds.; Woodhead Publishing Ltd.: Cambridge, UK, 2009; pp. 25–68.
16. Böhner, M. Calcium Orthophosphates in Medicine: From Ceramics to Calcium Phosphate Cements. *Injury* **2000**, *31* (Suppl. S4), 37–47. [\[CrossRef\]](#) [\[PubMed\]](#)
17. Tariq, U.; Haider, Z.; Chaudhary, K.; Hussain, R.; Ali, J. Calcium to phosphate ratio measurements in calcium phosphates using LIBS. *J. Phys. Conf. Ser.* **2018**, *1027*, 012015. [\[CrossRef\]](#)
18. Boushell, M.K.; Khanarian, N.T.; LeGeros, R.Z.; Lu, H.H. Effect of Ceramic Calcium Phosphorus Ratio on Chondrocyte-Mediated Biosynthesis and Mineralization. *J. Biomed. Mater. Res. A* **2017**, *105*, 2694–2702. [\[CrossRef\]](#) [\[PubMed\]](#)
19. Wang, B.; Zhang, Z.; Pan, H. Bone Apatite Nanocrystal: Crystalline Structure, Chemical Composition, and Architecture. *Biomimetics* **2023**, *8*, 90. [\[CrossRef\]](#) [\[PubMed\]](#)
20. Beniash, E. Biomaterials—Hierarchical Nanocomposites: The Example of Bone. *Wiley Interdiscip. Rev. Nanomed. Nanobiotechnol.* **2011**, *3*, 47–69. [\[CrossRef\]](#)
21. Georgiadis, M.; Müller, R.; Schneider, P. Techniques to Assess Bone Ultrastructure Organization: Orientation and Arrangement of Mineralized Collagen Fibrils. *J. R. Soc. Interface* **2016**, *13*, 20160088. [\[CrossRef\]](#)
22. Ielo, I.; Calabrese, G.; De Luca, G.; Conoci, S. Recent Advances in Hydroxyapatite-Based Biocomposites for Bone Tissue Regeneration in Orthopedics. *Int. J. Mol. Sci.* **2022**, *23*, 9721. [\[CrossRef\]](#) [\[PubMed\]](#)
23. Al-Qudsy, L.; Hu, Y.W.; Xu, H.; Yang, P.F. Mineralized Collagen Fibrils: An Essential Component in Determining the Mechanical Behavior of Cortical Bone. *ACS Biomater. Sci. Eng.* **2023**, *9*, 2203–2219. [\[CrossRef\]](#) [\[PubMed\]](#)
24. Hara, E.S.; Okada, M.; Nagaoka, N.; Nakano, T.; Matsumoto, T. Re-Evaluation of Initial Bone Mineralization from an Engineering Perspective. *Tissue Eng. Part B Rev.* **2022**, *28*, 246–255. [\[CrossRef\]](#) [\[PubMed\]](#)
25. Ma, C.; Du, T.; Niu, X.; Fan, Y. Biomechanics and Mechanobiology of the Bone Matrix. *Bone Res.* **2022**, *10*, 95. [\[CrossRef\]](#) [\[PubMed\]](#)
26. Uludag, H.; Gao, T.; Porter, T.; Friess, W.; Wozney, J. Delivery Systems for BMPs: Factors Contributing to Protein Retention at an Application Site. *J. Bone Jt. Surg. Am.* **2001**, *83*, S128–S135. [\[CrossRef\]](#)
27. Uludag, H.; D’Augusta, D.; Golden, J.L.; Timony, G.; Riedel, R.; Wozney, J.M. Implantation of Recombinant Human Bone Morphogenetic Proteins with Biomaterial Carriers: A Correlation between Protein Pharmacokinetics and Osteoinduction in the Rat Ectopic Model. *J. Biomed. Mater. Res.* **2000**, *50*, 227–238. [\[CrossRef\]](#)
28. Huang, R.L.; Yuan, Y.; Tu, J.; Zou, G.M.; Li, Q. Exaggerated Inflammatory Environment Decreases BMP-2/ACS-Induced Ectopic Bone Mass in a Rat Model: Implications for Clinical Use of BMP-2. *Osteoarthr. Cartil.* **2014**, *22*, 1186–1196. [\[CrossRef\]](#) [\[PubMed\]](#)

29. Geiger, M.; Li, R.H.; Friess, W. Collagen Sponges for Bone Regeneration with RhBMP-2. *Adv. Drug Deliv. Rev.* **2003**, *55*, 1613–1629. [[CrossRef](#)] [[PubMed](#)]
30. Friess, W.; Uludag, H.; Foskett, S.; Biron, R.; Sargeant, C. Characterization of Absorbable Collagen Sponges as Recombinant Human Bone Morphogenetic Protein-2 Carriers. *Int. J. Pharm.* **1999**, *185*, 51–60. [[CrossRef](#)]
31. Miyazaki, M.; Morishita, Y.; He, W.; Hu, M.; Sintuu, C.; Hymanson, H.J.; Falakassa, J.; Tsumura, H.; Wang, J.C. A Porcine Collagen-Derived Matrix as a Carrier for Recombinant Human Bone Morphogenetic Protein-2 Enhances Spinal Fusion in Rats. *Spine J.* **2009**, *9*, 22–30. [[CrossRef](#)]
32. Cho, T.H.; Kim, I.S.; Lee, B.; Park, S.N.; Ko, J.H.; Hwang, S.J. Early and Marked Enhancement of New Bone Quality by Alendronate-Loaded Collagen Sponge Combined with Bone Morphogenetic Protein-2 at High Dose: A Long-Term Study in Calvarial Defects in a Rat Model. *Tissue Eng. Part A* **2017**, *23*, 1343–1360. [[CrossRef](#)] [[PubMed](#)]
33. Pelaez, M.; Susin, C.; Lee, J.; Fiorini, T.; Bisch, F.C.; Dixon, D.R.; McPherson, J.C.; Buxton, A.N.; Wikesjö, U.M.E. Effect of RhBMP-2 Dose on Bone Formation/Maturation in a Rat Critical-Size Calvarial Defect Model. *J. Clin. Periodontol.* **2014**, *41*, 827–836. [[CrossRef](#)] [[PubMed](#)]
34. Kato, M.; Toyoda, H.; Namikawa, T.; Hoshino, M.; Terai, H.; Miyamoto, S.; Takaoka, K. Optimized Use of a Biodegradable Polymer as a Carrier Material for the Local Delivery of Recombinant Human Bone Morphogenetic Protein-2 (RhBMP-2). *Biomaterials* **2006**, *27*, 2035–2041. [[CrossRef](#)] [[PubMed](#)]
35. Chen, Z.; Zhang, Z.; Ma, X.; Duan, Z.; Hui, J.; Zhu, C.; Zhang, D.; Fan, D.; Shang, L.; Chen, F. Newly Designed Human-Like Collagen to Maximize Sensitive Release of BMP-2 for Remarkable Repairing of Bone Defects. *Biomolecules* **2019**, *9*, 450. [[CrossRef](#)] [[PubMed](#)]
36. Nakamura, T.; Shirakata, Y.; Shinohara, Y.; Miron, R.J.; Furue, K.; Noguchi, K. Osteogenic Potential of Recombinant Human Bone Morphogenetic Protein-9/Absorbable Collagen Sponge (RhBMP-9/ACS) in Rat Critical Size Calvarial Defects. *Clin. Oral Investig.* **2017**, *21*, 1659–1665. [[CrossRef](#)] [[PubMed](#)]
37. Nam, J.W.; Kim, H.J. Stepwise Verification of Bone Regeneration Using Recombinant Human Bone Morphogenetic Protein-2 in Rat Fibula Model. *J. Korean Assoc. Oral Maxillofac. Surg.* **2017**, *43*, 373–387. [[CrossRef](#)] [[PubMed](#)]
38. Fujioka-Kobayashi, M.; Abd El Raouf, M.; Saulacic, N.; Kobayashi, E.; Zhang, Y.; Schaller, B.; Miron, R.J. Superior Bone-Inducing Potential of RhBMP9 Compared to RhBMP2. *J. Biomed. Mater. Res. A* **2018**, *106*, 1561–1574. [[CrossRef](#)] [[PubMed](#)]
39. Pang, E.-K.; Im, S.-U.; Kim, C.-S.; Choi, S.-H.; Chai, J.-K.; Kim, C.-K.; Han, S.-B.; Cho, K.-S. Effect of Recombinant Human Bone Morphogenetic Protein-4 Dose on Bone Formation in a Rat Calvarial Defect Model. *J. Periodontol.* **2004**, *75*, 1364–1370. [[CrossRef](#)] [[PubMed](#)]
40. Kim, C.S.; Il Kim, J.; Kim, J.; Choi, S.H.; Chai, J.K.; Kim, C.K.; Cho, K.S. Ectopic Bone Formation Associated with Recombinant Human Bone Morphogenetic Proteins-2 Using Absorbable Collagen Sponge and Beta Tricalcium Phosphate as Carriers. *Biomaterials* **2005**, *26*, 2501–2507. [[CrossRef](#)]
41. Omura, S.; Mizuki, N.; Kawabe, R.; Ota, S.; Kobayashi, S.; Fujita, K. A Carrier for Clinical Use of Recombinant Human BMP-2: Dehydrothermally Cross-Linked Composite of Fibrillar and Denatured Atelocollagen Sponge. *Int. J. Oral Maxillofac. Surg.* **1998**, *27*, 129–134. [[CrossRef](#)]
42. Yamamoto, M.; Takahashi, Y.; Tabata, Y. Controlled Release by Biodegradable Hydrogels Enhances the Ectopic Bone Formation of Bone Morphogenetic Protein. *Biomaterials* **2003**, *24*, 4375–4383. [[CrossRef](#)]
43. Saito, A.; Suzuki, Y.; Ogata, S.I.; Ohtsuki, C.; Tanihara, M. Prolonged Ectopic Calcification Induced by BMP-2-Derived Synthetic Peptide. *J. Biomed. Mater. Res. A* **2004**, *70*, 115–121. [[CrossRef](#)] [[PubMed](#)]
44. Zhang, H.; Yang, L.; Yang, X.G.; Wang, F.; Feng, J.T.; Hua, K.C.; Li, Q.; Hu, Y.-C. Demineralized Bone Matrix Carriers and Their Clinical Applications: An Overview. *Orthop. Surg.* **2019**, *11*, 725–737. [[CrossRef](#)]
45. Tsiroidis, E.; Ali, Z.; Bhalla, A.; Heliotis, M.; Gurav, N.; Deb, S.; DiSilvio, L. In Vitro and in Vivo Optimization of Impaction Allografting by Demineralization and Addition of Rh-OP-1. *J. Orthop. Res.* **2007**, *25*, 1425–1437. [[CrossRef](#)] [[PubMed](#)]
46. Klotz, B.J.; Gawlitta, D.; Rosenberg, A.J.W.P.; Malda, J.; Melchels, F.P.W. Gelatin-Methacryloyl Hydrogels: Towards Biofabrication-Based Tissue Repair. *Trends Biotechnol.* **2016**, *34*, 394–407. [[CrossRef](#)] [[PubMed](#)]
47. Islam, M.M.; Khan, M.A.; Rahman, M.M. Preparation of Gelatin Based Porous Biocomposite for Bone Tissue Engineering and Evaluation of Gamma Irradiation Effect on Its Properties. *Mater. Sci. Eng. C Mater. Biol. Appl.* **2015**, *49*, 648–655. [[CrossRef](#)]
48. Yang, G.; Xiao, Z.; Long, H.; Ma, K.; Zhang, J.; Ren, X.; Zhang, J. Assessment of the Characteristics and Biocompatibility of Gelatin Sponge Scaffolds Prepared by Various Crosslinking Methods. *Sci. Rep.* **2018**, *8*, 1616. [[CrossRef](#)]
49. Takahashi, Y.; Yamamoto, M.; Tabata, Y. Enhanced Osteoinduction by Controlled Release of Bone Morphogenetic Protein-2 from Biodegradable Sponge Composed of Gelatin and Beta-Tricalcium Phosphate. *Biomaterials* **2005**, *26*, 4856–4865. [[CrossRef](#)] [[PubMed](#)]
50. Saito, A.; Suzuki, Y.; Ogata, S.I.; Ohtsuki, C.; Tanihara, M. Activation of Osteo-Progenitor Cells by a Novel Synthetic Peptide Derived from the Bone Morphogenetic Protein-2 Knuckle Epitope. *Biochim. Biophys. Acta* **2003**, *1651*, 60–67. [[CrossRef](#)]
51. Saito, A.; Suzuki, Y.; Ogata, S.I.; Ohtsuki, C.; Tanihara, M. Accelerated Bone Repair with the Use of a Synthetic BMP-2-Derived Peptide and Bone-Marrow Stromal Cells. *J. Biomed. Mater. Res. A* **2005**, *72*, 77–82. [[CrossRef](#)]
52. Saito, A.; Suzuki, Y.; Kitamura, M.; Ogata, S.I.; Yoshihara, Y.; Masuda, S.; Ohtsuki, C.; Tanihara, M. Repair of 20-Mm Long Rabbit Radial Bone Defects Using BMP-Derived Peptide Combined with an α -Tricalcium Phosphate Scaffold. *J. Biomed. Mater. Res. A* **2006**, *77*, 700–706. [[CrossRef](#)] [[PubMed](#)]

53. Simmons, C.A.; Alsberg, E.; Hsiong, S.; Kim, W.J.; Mooney, D.J. Dual Growth Factor Delivery and Controlled Scaffold Degradation Enhance in Vivo Bone Formation by Transplanted Bone Marrow Stromal Cells. *Bone* **2004**, *35*, 562–569. [\[CrossRef\]](#) [\[PubMed\]](#)
54. Boerckel, J.D.; Kolambkar, Y.M.; Dupont, K.M.; Uhrig, B.A.; Phelps, E.A.; Stevens, H.Y.; García, A.J.; Guldberg, R.E. Effects of Protein Dose and Delivery System on BMP-Mediated Bone Regeneration. *Biomaterials* **2011**, *32*, 5241–5251. [\[CrossRef\]](#) [\[PubMed\]](#)
55. Krishnan, L.; Priddy, L.B.; Esancy, C.; Klosterhoff, B.S.; Stevens, H.Y.; Tran, L.; Guldberg, R.E. Delivery Vehicle Effects on Bone Regeneration and Heterotopic Ossification Induced by High Dose BMP-2. *Acta Biomater.* **2017**, *49*, 101–112. [\[CrossRef\]](#) [\[PubMed\]](#)
56. Krishnan, L.; Priddy, L.B.; Esancy, C.; Li, M.T.A.; Stevens, H.Y.; Jiang, X.; Tran, L.; Rowe, D.W.; Guldberg, R.E. Hydrogel-Based Delivery of RhBMP-2 Improves Healing of Large Bone Defects Compared with Autograft. *Clin. Orthop. Relat. Res.* **2015**, *473*, 2885–2897. [\[CrossRef\]](#) [\[PubMed\]](#)
57. Kowalczewski, C.J.; Saul, J.M. Biomaterials for the Delivery of Growth Factors and Other Therapeutic Agents in Tissue Engineering Approaches to Bone Regeneration. *Front. Pharmacol.* **2018**, *9*, 513. [\[CrossRef\]](#) [\[PubMed\]](#)
58. Luca, L.; Rougemont, A.L.; Walpoth, B.H.; Boure, L.; Tami, A.; Anderson, J.M.; Jordan, O.; Gurny, R. Injectable RhBMP-2-Loaded Chitosan Hydrogel Composite: Osteoinduction at Ectopic Site and in Segmental Long Bone Defect. *J. Biomed. Mater. Res. A* **2011**, *96*, 66–74. [\[CrossRef\]](#) [\[PubMed\]](#)
59. Venkatesan, J.; Anil, S.; Kim, S.K.; Shim, M.S. Chitosan as a Vehicle for Growth Factor Delivery: Various Preparations and Their Applications in Bone Tissue Regeneration. *Int. J. Biol. Macromol.* **2017**, *104*, 1383–1397. [\[CrossRef\]](#) [\[PubMed\]](#)
60. Bakopoulou, A.; Georgopoulou, A.; Grivas, I.; Bekiari, C.; Prymak, O.; Loza, K.; Epple, M.; Papadopoulos, G.C.; Koidis, P.; Chatzinikolaïdou, M. Dental Pulp Stem Cells in Chitosan/Gelatin Scaffolds for Enhanced Orofacial Bone Regeneration. *Dent. Mater.* **2019**, *35*, 310–327. [\[CrossRef\]](#)
61. Park, D.J.; Choi, B.H.; Zhu, S.J.; Huh, J.Y.; Kim, B.Y.; Lee, S.H. Injectable Bone Using Chitosan-Alginate Gel/Mesenchymal Stem Cells/BMP-2 Composites. *J. Craniomaxillofac. Surg.* **2005**, *33*, 50–54. [\[CrossRef\]](#)
62. Bulpitt, P.; Aeschlimann, D. New Strategy for Chemical Modification of Hyaluronic Acid: Preparation of Functionalized Derivatives and Their Use in the Formation of Novel Biocompatible Hydrogels. *J. Biomed. Mater. Res.* **1999**, *47*, 152–169. [\[CrossRef\]](#)
63. Bhakta, G.; Lim, Z.X.H.; Rai, B.; Lin, T.; Hui, J.H.; Prestwich, G.D.; Van Wijnen, A.J.; Nurcombe, V.; Cool, S.M. The Influence of Collagen and Hyaluronan Matrices on the Delivery and Bioactivity of Bone Morphogenetic Protein-2 and Ectopic Bone Formation. *Acta Biomater.* **2013**, *9*, 9098–9106. [\[CrossRef\]](#) [\[PubMed\]](#)
64. Bhakta, G.; Rai, B.; Lim, Z.X.H.; Hui, J.H.; Stein, G.S.; van Wijnen, A.J.; Nurcombe, V.; Prestwich, G.D.; Cool, S.M. Hyaluronic Acid-Based Hydrogels Functionalized with Heparin That Support Controlled Release of Bioactive BMP-2. *Biomaterials* **2012**, *33*, 6113–6122. [\[CrossRef\]](#)
65. Arosarena, O.; Collins, W. Comparison of BMP-2 and -4 for Rat Mandibular Bone Regeneration at Various Doses. *Orthod. Craniofac. Res.* **2005**, *8*, 267–276. [\[CrossRef\]](#)
66. Eckardt, H.; Christensen, K.S.; Lind, M.; Hansen, E.S.; Hall, D.W.R.; Hvid, I. Recombinant Human Bone Morphogenetic Protein 2 Enhances Bone Healing in an Experimental Model of Fractures at Risk of Non-Union. *Injury* **2005**, *36*, 489–494. [\[CrossRef\]](#) [\[PubMed\]](#)
67. Kim, J.; Kim, I.S.; Cho, T.H.; Lee, K.B.; Hwang, S.J.; Tae, G.; Noh, I.; Lee, S.H.; Park, Y.; Sun, K. Bone Regeneration Using Hyaluronic Acid-Based Hydrogel with Bone Morphogenetic Protein-2 and Human Mesenchymal Stem Cells. *Biomaterials* **2007**, *28*, 1830–1837. [\[CrossRef\]](#)
68. Maire, M.; Chaubet, F.; Mary, P.; Blanchat, C.; Meunier, A.; Logeart-Avramoglou, D. Bovine BMP Osteoinductive Potential Enhanced by Functionalized Dextran-Derived Hydrogels. *Biomaterials* **2005**, *26*, 5085–5092. [\[CrossRef\]](#) [\[PubMed\]](#)
69. Schützenberger, S.; Schultz, A.; Hausner, T.; Hopf, R.; Zanoni, G.; Morton, T.; Kropik, K.; Van Griensven, M.; Redl, H. The Optimal Carrier for BMP-2: A Comparison of Collagen versus Fibrin Matrix. *Arch. Orthop. Trauma Surg.* **2012**, *132*, 1363–1370. [\[CrossRef\]](#)
70. Han, D.-K.; Kim, C.-S.; Jung, U.-W.; Chai, J.-K.; Choi, S.-H.; Kim, C.-K.; Cho, K.-S. Effect of a Fibrin-Fibronectin Sealing System as a Carrier for Recombinant Human Bone Morphogenetic Protein-4 on Bone Formation in Rat Calvarial Defects. *J. Periodontol.* **2005**, *76*, 2216–2222. [\[CrossRef\]](#)
71. Zhu, S.J.; Choi, B.H.; Jung, J.H.; Lee, S.H.; Huh, J.Y.; You, T.M.; Lee, H.J.; Li, J. A Comparative Histologic Analysis of Tissue-Engineered Bone Using Platelet-Rich Plasma and Platelet-Enriched Fibrin Glue. *Oral Surg. Oral Med. Oral Pathol. Oral Radiol. Endod.* **2006**, *102*, 175–179. [\[CrossRef\]](#)
72. Pereira, H.F.; Cengiz, I.F.; Silva, F.S.; Reis, R.L.; Oliveira, J.M. Scaffolds and Coatings for Bone Regeneration. *J. Mater. Sci. Mater. Med.* **2020**, *31*, 27. [\[CrossRef\]](#) [\[PubMed\]](#)
73. Kirker-Head, C.; Karageorgiou, V.; Hofmann, S.; Fajardo, R.; Betz, O.; Merkle, H.P.; Hilbe, M.; von Rechenberg, B.; McCool, J.; Abrahamsen, L.; et al. BMP-Silk Composite Matrices Heal Critically Sized Femoral Defects. *Bone* **2007**, *41*, 247–255. [\[CrossRef\]](#)
74. Ghassemi, T.; Shahroodi, A.; Ebrahimzadeh, M.H.; Mousavian, A.; Movaffagh, J.; Moradi, A. Current Concepts in Scaffolding for Bone Tissue Engineering. *Arch. Bone Jt. Surg.* **2018**, *6*, 90–99.
75. Patel, J.J.; Flanagan, C.L.; Hollister, S.J. Bone Morphogenetic Protein-2 Adsorption onto Poly-ε-Caprolactone Better Preserves Bioactivity In Vitro and Produces More Bone In Vivo than Conjugation Under Clinically Relevant Loading Scenarios. *Tissue Eng. Part C Methods* **2015**, *21*, 489–498. [\[CrossRef\]](#) [\[PubMed\]](#)
76. Perez, R.A.; Mestres, G. Role of Pore Size and Morphology in Musculo-Skeletal Tissue Regeneration. *Mater. Sci. Eng. C Mater. Biol. Appl.* **2016**, *61*, 922–939. [\[CrossRef\]](#) [\[PubMed\]](#)

77. Karageorgiou, V.; Kaplan, D. Porosity of 3D Biomaterial Scaffolds and Osteogenesis. *Biomaterials* **2005**, *26*, 5474–5491. [[CrossRef](#)] [[PubMed](#)]
78. Tsuruga, E.; Takita, H.; Itoh, H.; Wakisaka, Y.; Kuboki, Y. Pore Size of Porous Hydroxyapatite as the Cell-Substratum Controls BMP-Induced Osteogenesis. *J. Biochem.* **1997**, *121*, 317–324. [[CrossRef](#)]
79. Chang, P.C.; Liu, B.Y.; Liu, C.M.; Chou, H.H.; Ho, M.H.; Liu, H.C.; Wang, D.M.; Hou, L.T. Bone Tissue Engineering with Novel RhBMP2-PLLA Composite Scaffolds. *J. Biomed. Mater. Res. A* **2007**, *81*, 771–780. [[CrossRef](#)]
80. Lee, S.H.; Shin, H. Matrices and Scaffolds for Delivery of Bioactive Molecules in Bone and Cartilage Tissue Engineering. *Adv. Drug Deliv. Rev.* **2007**, *59*, 339–359. [[CrossRef](#)]
81. Chen, Z.; Zhang, Z.; Feng, J.; Guo, Y.; Yu, Y.; Cui, J.; Li, H.; Shang, L. Influence of Mussel-Derived Bioactive BMP-2-Decorated PLA on MSC Behavior in Vitro and Verification with Osteogenicity at Ectopic Sites in Vivo. *ACS Appl. Mater. Interfaces* **2018**, *10*, 11961–11971. [[CrossRef](#)]
82. Jeon, O.; Song, S.J.; Kang, S.W.; Putnam, A.J.; Kim, B.S. Enhancement of Ectopic Bone Formation by Bone Morphogenetic Protein-2 Released from a Heparin-Conjugated Poly(L-Lactic-Co-Glycolic Acid) Scaffold. *Biomaterials* **2007**, *28*, 2763–2771. [[CrossRef](#)]
83. Hollinger, J.; Mayer, M.; Buck, D.; Zegzula, H.; Ron, E.; Smith, J.; Jin, L.; Wozney, J. Poly(α -Hydroxy Acid) Carrier for Delivering Recombinant Human Bone Morphogenetic Protein-2 for Bone Regeneration. *J. Control. Release* **1996**, *39*, 287–304. [[CrossRef](#)]
84. Lutolf, M.P.; Lauer-Fields, J.L.; Schmoekel, H.G.; Metters, A.T.; Weber, F.E.; Fields, G.B.; Hubbell, J.A. Synthetic Matrix Metalloproteinase-Sensitive Hydrogels for the Conduction of Tissue Regeneration: Engineering Cell-Invasion Characteristics. *Proc. Natl. Acad. Sci. USA* **2003**, *100*, 5413–5418. [[CrossRef](#)]
85. Lutolf, M.P.; Weber, F.E.; Schmoekel, H.G.; Schense, J.C.; Kohler, T.; Müller, R.; Hubbell, J.A. Repair of Bone Defects Using Synthetic Mimetics of Collagenous Extracellular Matrices. *Nat. Biotechnol.* **2003**, *21*, 513–518. [[CrossRef](#)]
86. Vallmajo-Martin, Q.; Millan, C.; Müller, R.; Weber, F.E.; Ehrbar, M.; Ghayor, C. Enhanced bone regeneration in rat calvarial defects through BMP2 release from engineered poly(ethylene glycol) hydrogels. *Sci. Rep.* **2024**, *14*, 4916. [[CrossRef](#)] [[PubMed](#)]
87. Suzuki, A.; Terai, H.; Toyoda, H.; Namikawa, T.; Yokota, Y.; Tsunoda, T.; Takaoka, K. A Biodegradable Delivery System for Antibiotics and Recombinant Human Bone Morphogenetic Protein-2: A Potential Treatment for Infected Bone Defects. *J. Orthop. Res.* **2006**, *24*, 327–332. [[CrossRef](#)] [[PubMed](#)]
88. Kirker-Head, C.A. Potential Applications and Delivery Strategies for Bone Morphogenetic Proteins. *Adv. Drug Deliv. Rev.* **2000**, *43*, 65–92. [[CrossRef](#)] [[PubMed](#)]
89. Murata, M.; Inoue, M.; Arisue, M.; Kuboki, Y.; Nagai, N. Carrier-Dependency of Cellular Differentiation Induced by Bone Morphogenetic Protein in Ectopic Sites. *Int. J. Oral Maxillofac. Surg.* **1998**, *27*, 391–396. [[CrossRef](#)] [[PubMed](#)]
90. Noshi, T.; Yoshikawa, T.; Dohi, Y.; Ikeuchi, M.; Horiuchi, K.; Ichijima, K.; Sugimura, M.; Yonemasu, K.; Ohgushi, H. Recombinant Human Bone Morphogenetic Protein-2 Potentiates the in Vivo Osteogenic Ability of Marrow/Hydroxyapatite Composites. *Artif. Organs* **2001**, *25*, 201–208. [[CrossRef](#)]
91. Liang, G.; Yang, Y.; Oh, S.; Ong, J.L.; Zheng, C.; Ran, J.; Yin, G.; Zhou, D. Ectopic Osteoinduction and Early Degradation of Recombinant Human Bone Morphogenetic Protein-2-Loaded Porous Beta-Tricalcium Phosphate in Mice. *Biomaterials* **2005**, *26*, 4265–4271. [[CrossRef](#)]
92. Kohara, H.; Tabata, Y. Enhancement of Ectopic Osteoid Formation Following the Dual Release of Bone Morphogenetic Protein 2 and Wnt1 Inducible Signaling Pathway Protein 1 from Gelatin Sponges. *Biomaterials* **2011**, *32*, 5726–5732. [[CrossRef](#)] [[PubMed](#)]
93. Fujita, N.; Matsushita, T.; Ishida, K.; Sasaki, K.; Kubo, S.; Matsumoto, T.; Kurosaka, M.; Tabata, Y.; Kuroda, R. An Analysis of Bone Regeneration at a Segmental Bone Defect by Controlled Release of Bone Morphogenetic Protein 2 from a Biodegradable Sponge Composed of Gelatin and β -Tricalcium Phosphate. *J. Tissue Eng. Regen. Med.* **2012**, *6*, 291–298. [[CrossRef](#)] [[PubMed](#)]
94. Yamamoto, M.; Hokugo, A.; Takahashi, Y.; Nakano, T.; Hiraoka, M.; Tabata, Y. Combination of BMP-2-Releasing Gelatin/ β -TCP Sponges with Autologous Bone Marrow for Bone Regeneration of X-Ray-Irradiated Rabbit Ulner Defects. *Biomaterials* **2015**, *56*, 18–25. [[CrossRef](#)] [[PubMed](#)]
95. Tsiridis, E.; Morgan, E.F.; Bancroft, J.M.; Song, M.; Kain, M.; Gerstenfeld, L.; Einhorn, T.A.; Bouxsein, M.L.; Tornetta, P. Effects of OP-1 and PTH in a New Experimental Model for the Study of Metaphyseal Bone Healing. *J. Orthop. Res.* **2007**, *25*, 1193–1203. [[CrossRef](#)] [[PubMed](#)]
96. Susin, C.; Lee, J.; Fiorini, T.; De Freitas, R.M.; Chiu, H.C.; Prasad, H.S.; Buxton, A.N.; Wikesjö, U.M.E. Sinus Augmentation Using RhBMP-2/ACS in a Mini-Pig Model: Influence of an Adjunctive Ceramic Bone Biomaterial. *J. Clin. Periodontol.* **2018**, *45*, 1005–1013. [[CrossRef](#)] [[PubMed](#)]
97. Arosarena, O.A.; Collins, W.L. Bone Regeneration in the Rat Mandible with Bone Morphogenetic Protein-2: A Comparison of Two Carriers. *Otolaryngol. Head Neck Surg.* **2005**, *132*, 592–597. [[CrossRef](#)] [[PubMed](#)]
98. Quinlan, E.; Thompson, E.M.; Matsiko, A.; O'Brien, F.J.; López-Noriega, A. Long-Term Controlled Delivery of RhBMP-2 from Collagen-Hydroxyapatite Scaffolds for Superior Bone Tissue Regeneration. *J. Control. Release* **2015**, *207*, 112–119. [[CrossRef](#)]
99. Wang, Y.J.; Lin, F.H.; Sun, J.S.; Huang, Y.C.; Chueh, S.C.; Hsu, F.Y. Collagen-Hydroxyapatite Microspheres as Carriers for Bone Morphogenetic Protein-4. *Artif. Organs* **2003**, *27*, 162–168. [[CrossRef](#)] [[PubMed](#)]
100. Hussain, A.; Takahashi, K.; Sonobe, J.; Tabata, Y.; Bessho, K. Bone Regeneration of Rat Calvarial Defect by Magnesium Calcium Phosphate Gelatin Scaffolds with or without Bone Morphogenetic Protein-2. *J. Maxillofac. Oral Surg.* **2014**, *13*, 29–35. [[CrossRef](#)]

101. Raina, D.B.; Larsson, D.; Mrkonjic, F.; Isaksson, H.; Kumar, A.; Lidgren, L.; Tägil, M. Gelatin- Hydroxyapatite- Calcium Sulphate Based Biomaterial for Long Term Sustained Delivery of Bone Morphogenic Protein-2 and Zoledronic Acid for Increased Bone Formation: In-Vitro and in-Vivo Carrier Properties. *J. Control. Release* **2018**, *272*, 83–96. [[CrossRef](#)]
102. Kato, M.; Namikawa, T.; Terai, H.; Hoshino, M.; Miyamoto, S.; Takaoka, K. Ectopic Bone Formation in Mice Associated with a Lactic Acid/Dioxanone/Ethylene Glycol Copolymer-Tricalcium Phosphate Composite with Added Recombinant Human Bone Morphogenetic Protein-2. *Biomaterials* **2006**, *27*, 3927–3933. [[CrossRef](#)] [[PubMed](#)]
103. Matsushita, N.; Terai, H.; Okada, T.; Nozaki, K.; Inoue, H.; Miyamoto, S.; Takaoka, K. Accelerated Repair of a Bone Defect with a Synthetic Biodegradable Bone-Inducing Implant. *J. Orthop. Sci.* **2006**, *11*, 505–511. [[CrossRef](#)] [[PubMed](#)]
104. Yoneda, M.; Terai, H.; Imai, Y.; Okada, T.; Nozaki, K.; Inoue, H.; Miyamoto, S.; Takaoka, K. Repair of an Intercalated Long Bone Defect with a Synthetic Biodegradable Bone-Inducing Implant. *Biomaterials* **2005**, *26*, 5145–5152. [[CrossRef](#)] [[PubMed](#)]
105. Kaito, T.; Myoui, A.; Takaoka, K.; Saito, N.; Nishikawa, M.; Tamai, N.; Ohgushi, H.; Yoshikawa, H. Potentiation of the Activity of Bone Morphogenetic Protein-2 in Bone Regeneration by a PLA-PEG/Hydroxyapatite Composite. *Biomaterials* **2005**, *26*, 73–79. [[CrossRef](#)] [[PubMed](#)]
106. Murakami, N.; Saito, N.; Horiuchi, H.; Okada, T.; Nozaki, K.; Takaoka, K. Repair of Segmental Defects in Rabbit Humeri with Titanium Fiber Mesh Cylinders Containing Recombinant Human Bone Morphogenetic Protein-2 (RhBMP-2) and a Synthetic Polymer. *J. Biomed. Mater. Res.* **2002**, *62*, 169–174. [[CrossRef](#)] [[PubMed](#)]
107. Yokota, S.; Sonohara, S.; Yoshida, M.; Murai, M.; Shimokawa, S.; Fujimoto, R.; Fukushima, S.; Kokubo, S.; Nozaki, K.; Takahashi, K.; et al. A New Recombinant Human Bone Morphogenetic Protein-2 Carrier for Bone Regeneration. *Int. J. Pharm.* **2001**, *223*, 69–79. [[CrossRef](#)] [[PubMed](#)]
108. Kokubo, S.; Fujimoto, R.; Yokota, S.; Fukushima, S.; Nozaki, K.; Takahashi, K.; Miyata, K. Bone Regeneration by Recombinant Human Bone Morphogenetic Protein-2 and a Novel Biodegradable Carrier in a Rabbit Ulnar Defect Model. *Biomaterials* **2003**, *24*, 1643–1651. [[CrossRef](#)] [[PubMed](#)]
109. Olthof, M.G.L.; Tryfonidou, M.A.; Liu, X.; Pouran, B.; Meij, B.P.; Dhert, W.J.A.; Yaszemski, M.J.; Lu, L.; Alblas, J.; Kempen, D.H.R. Phosphate Functional Groups Improve Oligo[(Polyethylene Glycol) Fumarate] Osteoconduction and BMP-2 Osteoinductive Efficacy. *Tissue Eng. Part A* **2018**, *24*, 819–829. [[CrossRef](#)] [[PubMed](#)]
110. Lee, S.C.; Shea, M.; Battle, M.A.; Kozitza, K.; Ron, E.; Turek, T.; Schaub, R.G.; Hayes, W.C. Healing of Large Segmental Defects in Rat Femurs Is Aided by RhBMP-2 in PLGA Matrix. *J. Biomed. Mater. Res.* **1994**, *28*, 1149–1156. [[CrossRef](#)]
111. Irie, K.; Alpaslan, C.; Takahashi, K.; Kondo, Y.; Izumi, N.; Sakakura, Y.; Tsuruga, E.; Nakajima, T.; Ejiri, S.; Ozawa, H.; et al. Osteoclast Differentiation in Ectopic Bone Formation Induced by Recombinant Human Bone Morphogenetic Protein 2 (RhBMP-2). *J. Bone Miner. Metab.* **2003**, *21*, 363–369. [[CrossRef](#)]
112. Gan, Q.; Zhu, J.; Yuan, Y.; Liu, H.; Qian, J.; Li, Y.; Liu, C. A Dual-Delivery System of PH-Responsive Chitosan-Functionalized Mesoporous Silica Nanoparticles Bearing BMP-2 and Dexamethasone for Enhanced Bone Regeneration. *J. Mater. Chem. B* **2015**, *3*, 2056–2066. [[CrossRef](#)] [[PubMed](#)]
113. Zhou, X.; Feng, W.; Qiu, K.; Chen, L.; Wang, W.; Nie, W.; Mo, X.; He, C. BMP-2 Derived Peptide and Dexamethasone Incorporated Mesoporous Silica Nanoparticles for Enhanced Osteogenic Differentiation of Bone Mesenchymal Stem Cells. *ACS Appl. Mater. Interfaces* **2015**, *7*, 15777–15789. [[CrossRef](#)] [[PubMed](#)]
114. Mohammadi, M.; Alibolandi, M.; Abnous, K.; Salmasi, Z.; Jaafari, M.R.; Ramezani, M. Fabrication of Hybrid Scaffold Based on Hydroxyapatite-Biodegradable Nanofibers Incorporated with Liposomal Formulation of BMP-2 Peptide for Bone Tissue Engineering Fabrication of Hybrid Scaffold Based on Hydroxyapatite-Biodegradable Nanofibers Incorporated with Liposomal Formulation of BMP-2 Peptide for Bone Tissue Engineering. *Nanomedicine* **2018**, *14*, 1987–1997. [[PubMed](#)]
115. Li, X.; Zhang, R.; Tan, X.; Li, B.; Liu, Y.; Wang, X. Synthesis and Evaluation of BMMSC-Seeded BMP-6/NHAG/GMS Scaffolds for Bone Regeneration. *Int. J. Med. Sci.* **2019**, *16*, 1007–1017. [[CrossRef](#)] [[PubMed](#)]
116. Wei, G.; Jin, Q.; Giannobile, W.V.; Ma, P.X. The Enhancement of Osteogenesis by Nano-Fibrous Scaffolds Incorporating RhBMP-7 Nanospheres. *Biomaterials* **2007**, *28*, 2087–2096. [[CrossRef](#)] [[PubMed](#)]
117. Weng, L.; Boda, S.K.; Wang, H.; Teusink, M.J.; Shuler, F.D.; Xie, J. Novel 3D Hybrid Nanofiber Aerogels Coupled with BMP-2 Peptides for Cranial Bone Regeneration. *Adv. Healthc. Mater.* **2018**, *7*, e1701415. [[CrossRef](#)] [[PubMed](#)]
118. Chen, S.; Shi, Y.; Zhang, X.; Ma, J. Evaluation of BMP-2 and VEGF loaded 3D printed hydroxyapatite composite scaffolds with enhanced osteogenic capacity in vitro and in vivo. *Mater. Sci. Eng. C Mater. Biol. Appl.* **2020**, *112*, 110893. [[CrossRef](#)]
119. Helaelhil, J.V.; Lourenço, C.B.; Huang, B.; Helaelhil, L.V.; de Camargo, I.X.; Chiarotto, G.B.; Santamaria, M., Jr.; Bártolo, P.; Caetano, G.F. In Vivo Investigation of Polymer-Ceramic PCL/HA and PCL/ β -TCP 3D Composite Scaffolds and Electrical Stimulation for Bone Regeneration. *Polymers* **2021**, *14*, 65. [[CrossRef](#)]
120. Chan, J.K.C. The Wonderful Colors of the Hematoxylin-Eosin Stain in Diagnostic Surgical Pathology. *Int. J. Surg. Pathol.* **2014**, *22*, 12–32. [[CrossRef](#)]
121. Larson, K.; Ho, H.H.; Anumolu, P.L.; Chen, T.M. Hematoxylin and Eosin Tissue Stain in Mohs Micrographic Surgery: A Review. *Dermatol. Surg.* **2011**, *37*, 1089–1099. [[CrossRef](#)]
122. Rentsch, C.; Schneiders, W.; Manthey, S.; Rentsch, B.; Rammelt, S. Comprehensive Histological Evaluation of Bone Implants. *Biomatter* **2014**, *4*, e27993. [[CrossRef](#)] [[PubMed](#)]

123. Visser, R.; Bodnarova, K.; Arrabal, P.M.; Cifuentes, M.; Becerra, J. Combining Bone Morphogenetic Proteins-2 and -6 Has Additive Effects on Osteoblastic Differentiation in Vitro and Accelerates Bone Formation in Vivo. *J. Biomed. Mater. Res. A* **2016**, *104*, 178–185. [\[CrossRef\]](#)
124. Yang, R.; Davies, C.M.; Archer, C.W.; Richards, R.G.; Plenk, H.; Rooney, P.; Gasser, J. Immunohistochemistry of Matrix Markers in Technovit 9100 New-Embedded Undecalcified Bone Sections. *Eur Cell Mater* **2003**, *6*, 57–71. [\[CrossRef\]](#)
125. Luca, L.; Capelle, M.A.H.; Machaidze, G.; Arvinte, T.; Jordan, O.; Gurny, R. Physical Instability, Aggregation and Conformational Changes of Recombinant Human Bone Morphogenetic Protein-2 (RhBMP-2). *Int. J. Pharm.* **2010**, *391*, 48–54. [\[CrossRef\]](#)
126. Schneider, M.R. Von Kossa and His Staining Technique. *Histochem. Cell Biol.* **2021**, *156*, 523–526. [\[CrossRef\]](#) [\[PubMed\]](#)
127. Keene, D.R.; Tufa, S.F. Transmission Electron Microscopy of Cartilage and Bone. *Methods Cell Biol.* **2010**, *96*, 443–473. [\[PubMed\]](#)
128. Tallegas, M.; Gomez-Bouchet, A.; Legrand, M.; Bouvier, C.; de Pinieux, G. Markers for Bone Sarcomas. In *Bone Cancer: Bone Sarcomas and Bone Metastases—From Bench to Bedside*, 3rd ed.; Heymann, D., Ed.; Academic Press: Cambridge, MA, USA, 2022; pp. 543–577.
129. Fat, D.L.; Kennedy, J.; Galvin, R.; O'Brien, F.; Grath, F.M.; Mullett, H. The Hounsfield Value for Cortical Bone Geometry in the Proximal Humerus—An in Vitro Study. *Skelet. Radiol.* **2012**, *41*, 557–568.
130. Reuben, J.D.; Chang, C.H.; Akin, J.E.; Lionberger, D.R. A Knowledge-Based Computer-Aided Design and Manufacturing System for Total Hip Replacement. *Clin. Orthop. Relat. Res.* **1992**, *285*, 48–56. [\[CrossRef\]](#)
131. Aamodt, A.; Kvistad, K.A.; Andersen, E.; Lund-Larsen, J.; Eine, J.; Benum, P.; Husby, O.S. Determination of the Hounsfield Value for CT-Based Design of Custom Femoral Stems. *J. Bone Jt. Surg. Br.* **1999**, *81*, 143–147. [\[CrossRef\]](#)
132. Sukswai, N.; Khoury, J.D. Immunohistochemistry Innovations for Diagnosis and Tissue-Based Biomarker Detection. *Curr. Hematol. Malig. Rep.* **2019**, *14*, 368–375. [\[CrossRef\]](#)
133. Bonewald, L.F.; Harris, S.E.; Rosser, J.; Dallas, M.R.; Dallas, S.L.; Camacho, N.P.; Boyan, B.; Boskey, A. Von Kossa Staining Alone Is Not Sufficient to Confirm That Mineralization in Vitro Represents Bone Formation. *Calcif. Tissue Int.* **2003**, *72*, 537–547. [\[CrossRef\]](#)
134. MacMullan, P.; McMahon, G.; McCarthy, G. Detection of Basic Calcium Phosphate Crystals in Osteoarthritis. *Jt. Bone Spine* **2011**, *78*, 358–363. [\[CrossRef\]](#) [\[PubMed\]](#)
135. Sciau, P. Transmission Electron Microscopy: Emerging Investigations for Cultural Heritage Materials. *Adv. Imaging Electron. Phys.* **2016**, *198*, 43–67.
136. Brodusch, N.; Brahimi, S.V.; Barbosa De Melo, E.; Song, J.; Yue, S.; Piché, N.; Gauvin, R. Scanning Electron Microscopy versus Transmission Electron Microscopy for Material Characterization: A Comparative Study on High-Strength Steels. *Scanning* **2021**, *2021*, 5511618. [\[CrossRef\]](#)
137. Xue, B.; Li, Y.; Fu, Z.; Ping, H.; Wang, K. Intrafibrillar Growth of Hydroxyapatite Nanocrystals in Multiscale Collagen. *Crystals* **2023**, *13*, 692. [\[CrossRef\]](#)
138. Hornez, J.C.; Chai, F.; Monchau, F.; Blanchemain, N.; Descamps, M.; Hildebrand, H.F. Biological and Physico-Chemical Assessment of Hydroxyapatite (HA) with Different Porosity. *Biomol. Eng.* **2007**, *24*, 505–509. [\[CrossRef\]](#) [\[PubMed\]](#)
139. Raja, P.B.; Munusamy, K.R.; Perumal, V.; Ibrahim, M.N.M. Characterization of Nanomaterial Used in Nanobioremediation. In *Nano-Bioremediation: Fundamentals and Applications*; Iqbal, H.M., Bilal, M., Nguyen, T.A., Eds.; Elsevier: Amsterdam, The Netherlands, 2022; pp. 57–83.
140. Calafiori, A.R.; Di Marco, G.; Martino, G.; Marotta, M. Preparation and Characterization of Calcium Phosphate Biomaterials. *J. Mater. Sci. Mater. Med.* **2007**, *18*, 2331–2338. [\[CrossRef\]](#) [\[PubMed\]](#)
141. Cowan, C.M.; Soo, C.; Ting, K.; Wu, B. Evolving Concepts in Bone Tissue Engineering. *Curr. Top. Dev. Biol.* **2005**, *66*, 239–285. [\[PubMed\]](#)
142. Suzuki, Y.; Tanihara, M.; Suzuki, K.; Saitou, A.; Sufan, W.; Nishimura, Y. Alginate Hydrogel Linked with Synthetic Oligopeptide Derived from BMP-2 Allows Ectopic Osteoinduction in Vivo. *J. Biomed. Mater. Res.* **2000**, *50*, 405–409. [\[CrossRef\]](#)
143. Schmoekel, H.; Schense, J.C.; Weber, F.E.; Grätz, K.W.; Gnägi, D.; Müller, R.; Hubbell, J.A. Bone Healing in the Rat and Dog with Nonglycosylated BMP-2 Demonstrating Low Solubility in Fibrin Matrices. *J. Orthop. Res.* **2004**, *22*, 376–381. [\[CrossRef\]](#)
144. Schrier, J.A.; Fink, B.F.; Rodgers, J.B.; Vasconez, H.C.; DeLuca, P.P. Effect of a Freeze-Dried CMC/PLGA Microsphere Matrix of RhBMP-2 on Bone Healing. *AAPS PharmSciTech* **2001**, *2*, E18. [\[CrossRef\]](#) [\[PubMed\]](#)
145. Bedair, T.M.; Lee, C.K.; Kim, D.S.; Baek, S.W.; Bedair, H.M.; Joshi, H.P.; Choi, U.Y.; Park, K.H.; Park, W.; Han, I.; et al. Magnesium hydroxide-incorporated PLGA composite attenuates inflammation and promotes BMP2-induced bone formation in spinal fusion. *J. Tissue Eng.* **2020**, *11*, 2041731420967591. [\[CrossRef\]](#) [\[PubMed\]](#)
146. Cheng, R.; Yan, Y.; Liu, H.; Chen, H.; Pan, G.; Deng, L.; Cui, W. Mechanically Enhanced Lipo-Hydrogel with Controlled Release of Multi-Type Drugs for Bone Regeneration. *Appl. Mater. Today* **2018**, *12*, 294–308. [\[CrossRef\]](#)

Disclaimer/Publisher's Note: The statements, opinions and data contained in all publications are solely those of the individual author(s) and contributor(s) and not of MDPI and/or the editor(s). MDPI and/or the editor(s) disclaim responsibility for any injury to people or property resulting from any ideas, methods, instructions or products referred to in the content.